DEUTSCHES ELEKTRONEN-SYNCHROTRON **DESY**

DESY 79/71
October 1979

e^+e^- JETS

by

G. Schierholz

II. Institut für Theoretische Physik der Universität Hamburg

NOTKESTRASSE 85 · 2 HAMBURG 52

To be sure that your preprints are promptly included in the
HIGH ENERGY PHYSICS INDEX ,
send them to the following address (if possible by air mail) :

DESY
Bibliothek
Notkestrasse 85
2 Hamburg 52
Germany

DESY 79/71
October 1979

e^+e^- Jets *)

G. Schierholz

II. Institut für Theoretische Physik der Universität,

Hamburg

Invited talk given at the SLAC Summer Institute on Particle Physics, Topical Conference, 18-20 July, 1979.

*) Work supported by the German Bundesministerium für Forschung und Technologie and the U.S. Department of Energy under contract number DE - AC 03 - 76 SF 00515

1. Introduction

Quantum chromodynamics (QCD), the gauge theory of coloured quarks and gluons, is the only serious candidate for the theory of the strong interactions. It is not yet well understood as a field theory. E.g., the confinement problem is still in the dark, and we also do not know how to compute the hadron spectrum. But there is a large number of computable quantities and cross sections which can serve as tests and applications of QCD.

The classic application of QCD is to deep inelastic leptoproduction[1] where the short-distance expansion and the renormalization group are directly relevant. Other applications based on perturbation theory include jet cross sections in e^+e^- annihilation totally free of infrared singularities [2] - [5] and processes with universal infrared singularities which can be factored out[6], leaving the computable ultraviolet behaviour to be compared to experiment. Examples of the latter category are the Drell-Yan process[7][8], large-p_T hadron-hadron collisions and semi-inclusive leptoproduction and e^+e^- annihilation[9].

The status of QCD tests in deep inelastic lepton scattering has been reviewed by Barnett at this conference[10]. It appears that more data at higher q^2 are needed to provide discriminative tests of QCD. In particular, the presence of higher-twist contributions makes it impossible to unambiguously detect the logarithmic scaling violations and anomalous dimensions which distinguish QCD from alternative theories.

In order to put QCD on somewhat firmer grounds, it is essential to search for more direct signatures of coloured vector gluons (while evidence for the existence of elementary spin-1/2 quarks is abundant). In the first place this means to establish the quantum nature of glue. In place of free gluons

which are supposed to be confined, gluon jets originating in gluon bremsstrahlung off quarks and antiquarks (in conjunction with quark/antiquark jets) should best reflect the dynamics of coloured quarks and gluons at short distances.

At foreseeable energies deep inelastic leptoproduction will most likely not bring much of the gluon jets to light, mainly because the intrinsic transverse momentum of the constituent quarks, antiquarks and gluons (in the nucleon) washes out most of the effect[11]. Large-p_T proton-proton and pion-proton scattering at present accelerators are even less qualified to study gluon jets since this involves the intrinsic transverse momentum of both scattered partons. The most promising process to search for QCD jets is high-energy e^+e^- annihilation into hadrons, which is not spoiled by nonperturbative and (at present) intractable details of the initial state.

In this talk I shall concentrate on the application of QCD to e^+e^- annihilation into hadrons. Particular emphasis will be placed on QCD predictions which are reliably calculable and can soon be verified by experiment, i.e., which must not be affected by higher order corrections and nonperturbative effects and which are not just small effects on a much larger background.

In QCD high-energy e^+e^- annihilation cross sections which have no mass singularities can be calculated perturbatively[4)12)] with the fixed renormalized coupling constant replaced by the renormalization-group running coupling constant *)

$$\frac{\bar{g}^2}{4\pi} \equiv \alpha_s = \frac{12\pi}{(33-2N_f)\ln(q^2/\Lambda^2)} \qquad (1.1)$$

*) The running coupling constant quoted corresponds to the one-loop approximation.

with N_f the number of quark flavours and Λ to be determined experimentally. Since the running coupling constant vanishes for large q^2, generally only the first few terms of the perturbation series need to be calculated.

To order α_s^2, e^+e^- annihilation into hadrons is described by the diagrams*) listed in Fig. 1. The outgoing quarks, antiquarks and gluons, which appear to be confined in the real world, are assumed to metamorphose into hadrons with small transverse momentum**) ($\langle p_T \rangle$ = O(300 MeV)), i.e., jets. Accordingly, the predictions of perturbation theory for the production of quarks, antiquarks and gluons have to be interpreted as predictions for the production of jets.

The hypothesis that quarks and gluons fragment into hadrons with small transverse momentum is supported by QCD, using the absence of mass singularities as a criterion for the use of QCD perturbation theory. The cross section for e^+e^- multi-jet production events in which all but a fraction ε_i of the energy of the i-th jet is deposited inside a cone of half-angle δ_i was shown to be free of mass singularities[4)14)]. The result for the production of n quark, m antiquark and l gluon jets is ($\varepsilon_i \ll 1$, $\delta_i \ll 1$)

$$d\sigma_{jet}(nq+m\bar{q}+lg) = d\sigma_0(nq+m\bar{q}+lg)\left\{1-\frac{2\alpha_s}{\pi}\left[\sum_{i=1}^{n+m}\left(\ln\delta_i\ln\varepsilon_i + \frac{3}{4}\ln\delta_i\right) + 3\sum_{i=1}^{l}\left(\ln\delta_i\ln\varepsilon_i + \left(\frac{11}{6}-\frac{N_f}{4}\right)\ln\delta_i\right)\right]\right\}, \qquad (1.2)$$

where $d\sigma_0(nq + m\bar{q} + lg)$ is the cross section for $e^+e^- \to nq + m\bar{q} + lg$ in Born approximation. If we define a jet angular radius $\delta(\vartheta,\varepsilon)$ as in the two-jet case[4)], that is by requiring that a given fraction $1-\vartheta$, $\vartheta \ll 1$ of all events have at least $1-\varepsilon$ of the total energy emitted within n + m + l cones of half-angle $\delta(\vartheta,\varepsilon)$, we find that $\delta(\vartheta,\varepsilon) \to 0$ at high energies with some

*) ... corrections are not shown here.

power of $(1/q^2)$ as a result of $\alpha_s \to 0$. This demonstrates that the formation of jets is also a consequence of QCD.

Four jets are probably the maximum we can hope for to be seen at PETRA and PEP. Therefore we shall concentrate our discussion on singnatures of three- and four-jet final states, i.e., on the physics implemented by the diagrams shown in Fig. 1.

The jet cross section (1.2) is only one of a large class of cross sections which are free of mass singularities and are calculable in perturbation theory. Other measures of three- and four-jet final states, which will concern us here, are the differential cross sections in thrust[15] (T) and acoplanarity[5] (A) :

$$T = \max \left(\frac{\sum_i |p_{\parallel}^i|}{\sum_i |\vec{p}^{\,i}|} \right) , \qquad (1.3)$$

$$A = 4 \min \left(\frac{\sum_i |p_{out}^i|}{\sum_i |\vec{p}^{\,i}|} \right) , \qquad (1.4)$$

where the sum runs over all particles in the event and $p_{\parallel}^i$ (p_{out}^i) is measured parallel to the ("thrust") axis chosen to maximize T (perpendicular to the plane chosen to minimize A). A final state with $T \approx 1$ will correspond to two jets, while events with low thrust $T < 1$ should mostly consist of three jets. Acoplanarity, on the other hand, measures the deviation from disc-like events (i.e., three jets), so that a final state with nonvanishing $A > 0$ will mainly have a four-jet structure.

So far in the introduction emphasis was laid on the rather unambiguous predictions of asymptotically free QCD perturbation theory. This alone does, however, not give a complete picture. Some important tests of QCD such as quantum numbers (e.g. charge correlations), counting rules[16], polarization effects, etc. will

come from semi-inclusive processes. The question as to whether the inevitable infrared divergences and large logarithms of a naive application of perturbation theory to semi-inclusive processes can be handled has been answered yes[6]. The infrared divergences (also including mass singularities) factorize into separate universal infrared logarithms for each hadronic leg and ultraviolet logarithms . The infrared logarithms can be absorbed into the anyhow unknown fragmentation functions, where they actually belong, while the large ultraviolet logarithms arrange themselves so that the hard (parton) cross section can be re-expressed in terms of the running coupling constant α_s.

Over the last year, innumerable applications of perturbative QCD to e^+e^- annihilation have been presented. The question arises as to whether the proposed tests, when studied in alternate field theories, will give basically the same results as QCD or lead to different predictions. Only in the latter case could one speak of discriminative tests of QCD. As far as other theories are concerned, this rests, of course, on the assumption of a fixed point such that the effective coupling constant $\alpha_s^* \ll 1$. In this spirit I shall also discuss theories with scalar and pseudoscalar gluons.

If QCD proves to be the theory of the strong interactions, higher-twist contributions must also be present. They lead to quite similar effects as hard gluon bremsstrahlung and therefore should be watched out for if one is aiming at a quantitative test. Indeed, higher-twist contributions to e^+e^- annihilation have been estimated[17] and were found to be sizable even at higher PETRA and PEP energies. At given times I shall comment on higher-twist contributions*), especially, on how they can be discriminated. I feel that here some theoretical work needs to be done, in particular, as to their quantitative nature.

The talk is divided into two main parts. In Section 2 I shall discuss the application of (pure) QCD perturbation theory to the description of multi-jet

*) Which, by the way, also contain interesting physics.

final states including some remarks about heavy quark - antiquark pair production. In Section 3 I shall consider semi-inclusive processes. The topics discussed here are the transverse momentum profile of hadron jets and correlations. Section 4 contains a brief summary and outlook.

2. Multiple Jets (perturbative)

After Sterman and Weinberg[4] have paved the way, much interest has been devoted to jet calorimetry[14)18)-23)]. It has been found, however, that non-perturbative corrections are quite strong at PETRA and PEP energies and that the transition energy above which QCD effects start to dominate lies in the LEP region[24)]. This means that the proposed QCD tests in calorimeter experiments will have to wait for quite some time, so that we shall not discuss them here.

Three-Jet Final States

At low thrust the hadronic final state will basically have a three-jet structure (cf. Fig. 1 b) with a small admixture of four-jet events, etc. Perturbative QCD makes an absolute prediction for the tail of the thrust distribution*)[5)]

$$\frac{d\sigma}{dT} = \frac{2}{3}\frac{\alpha_s}{\pi}\sigma_0\left[\frac{2(3T^2-3T+2)}{T(1-T)}\ln\frac{2T-1}{1-T} - \frac{3(3T-2)(2-T)}{1-T}\right] + O(\alpha_s^2)\,. \tag{2.1}$$

For $T \to 1$ low-order perturbation theory is, however, not appropriate :

$$\frac{d\sigma}{dT}\underset{T\approx 1}{\approx}\frac{2}{3}\frac{\alpha_s}{\pi}\sigma_0\frac{4}{1-T}\left|\ln(1-T)\right|\,, \tag{2.2}$$

whereas we expect $d\sigma/dT \to 0$ for $T \to 1$. Here the effective expansion parameter is $(4\alpha_s/3\pi)\ln^2(1-T)$ which must be $\ll 1$ in order that finite order perturbation theory makes sense. The (infrared) singularity for $T \to 1$ in (2.1) and (2.2) is associated with soft and collinear gluon emission.

---

*) If not stated differently, quark masses will always be taken to be zero.

To all orders in the leading logarithm approximation ($\sim(\alpha_s \ln^2(1-T))^n$) the cross section is found to be *)

$$\frac{d\sigma}{dT} = \frac{8}{3}\frac{\alpha_s}{\pi}\sigma_0 \frac{|\ln(1-T)|}{1-T} e^{-\frac{4}{3}\frac{\alpha_s}{\pi}\ln^2(1-T)} . \qquad (2.3)$$

This is shown in Fig. 2 and compared to the lowest order contribution (2.1). As expected, (2.3) goes to zero for $T \to 1$, and it is indicated that (2.1) is (probably) applicable in the region $T \lesssim 0.9$, but definitely not beyond that.

The most serious nonperturbative background **) which might extend into the region of lower T comes from heavy quark-antiquark ($Q\bar{Q}$) pair production with subsequent decay. In Fig. 3 I have drawn $\sigma^{-1}\, d\sigma/dT$ (perturbative) together with a Monte Carlo calculation of the light [25] and heavy quark [26] background, respectively. At $\sqrt{q^2}$ = 30 GeV the effect of the b quark is already greatly shrunk back, and we expect to see a planar event structure for $T \lesssim 0.85$. For t production the signal is four times as large at scaled up energies and here would remain a serious background to gluon bremsstrahlung even far above threshold.

A complete kinematical determination of three-jet events requires two variables, apart from three Euler angles ***) fixing their orientation with respect to the beam and beam polarization axis. Besides T, the angle ϑ between the most

*) Details will be published elsewhere.

**) $\langle 1-T\rangle_{NP} \simeq (1/2)\,\langle n\rangle\,\langle p_T\rangle_{NP} / \sqrt{q^2}$ for light quarks and
$\langle 1-T\rangle_{NP} \simeq (\pi/4)\, m_Q / \sqrt{q^2}$ for heavy quarks.

***) Without polarization only two Euler angles are effective.

and second most energetic jet *) offers as the second variable. For a given T we obtain **)

$$\langle\cos\vartheta\rangle = 1 - 2\left[-3(2-T)(3T-2) + 6(2-T)(1-T)\ln\frac{2T}{2-T} + 2(2-3T+3T^2)\ln\frac{T^2}{(2-T)(1-T)}\right] \times \left[-3T(2-T)(3T-2) + 2(2-3T+3T^2)\ln\frac{2T-1}{1-T}\right]^{-1} . \qquad (2.4)$$

In particular,

T	$\langle\cos\vartheta\rangle$	ϑ	ϑ^*
0.7	-0.59	125.9^0	115.0^0
0.8	-0.79	142.0^0	98.3^0
0.9	-0.92	157.6^0	76.0^0
0.95	-0.97	166.2^0	58.7^0

(2.5)

where ϑ^* is the angle between the second most and least energetic jet, i.e., the minimal jet angle. The "typical" three-jet events corresponding to (2.5) are shown in Fig. 4. It should be noted that for T = 0.95, where Eq. (2.1) surely is not applicable anymore, ϑ^* is still much larger than the nonperturbative jet opening angle

$$\delta_{NP}^2 \approx \frac{\pi}{2}\frac{\langle n\rangle\langle p_T\rangle_{NP}}{\sqrt{q^2}} . \qquad (2.6)$$

*) Note that in the three-jet case the thrust axis coincides with the axis of the most energetic jet.

**) $\langle\cos\vartheta\rangle \to -1/2$ ($\vartheta = 120^0$) for $T \to 2/3$ and $\langle\cos\vartheta\rangle \to -1$ for $T \to 1$.

In order to fill this gap, higher order contributions will have to be included.

The quantitative test of QCD based on (2.1) now causes some problems. In order to determine T experimentally, one would have to measure neutrals. Furthermore, $d\sigma/dT$ is a steeply rising function of T, so that a small error in the measurement of T will ruin the precise determination of the cross section.

A test which appears to be rather clean is the production of jets at large angles *), i.e., in the center part of the Dalitz plot **) (Fig. 5). This involves measuring the rate of three-jet events with angles between some given $\vartheta_{min} > 0^o$ and $\vartheta_{max} < 180^o$. In Fig. 6 I have drawn ***) the cross section $d^2\sigma/d\vartheta d\vartheta^*$ on the borderlines ($\theta_2 = \theta_3$, $\theta_1 = \theta_3$; cf. Fig. 5) of the Dalitz plot. It shows that the cross section is rather flat within a reasonably large region $\vartheta_{min} \approx 80^o$, $\vartheta_{max} \approx 140^o$. This is the proviso for a quantitative test of QCD. Beyond that region the gluon jet is not guaranteed to be emitted at short distances and finite order perturbation theory breaks down. The latter is indicated by the sharp rise as $\vartheta \to 180^o$ and $\vartheta^* \to 0^o$.

In the following table I have listed the relative rate of expected (three-jet) events in various regions of the Dalitz plot

*) The relative jet angles taking over the role of T.

**) This is what Bjorken ever called the "gold-plated" test of QCD.

***) ϑ (ϑ^*) being, as before, the largest (smallest) relative jet angle.

	Rate	I
$\vartheta_{min} = 80^o$ $\vartheta_{max} = 140^o$	7.3 %	1.215
$\vartheta_{min} = 90^o$ $\vartheta_{max} = 135^o$	4.7 %	0.782
$\vartheta_{min} = 100^o$ $\vartheta_{max} = 130^o$	2.8 %	0.460

(2.7)

The parameters are $\sqrt{q^2} = 30$ GeV, $\Lambda = 0.5$ GeV, $N_f = 5$ which corresponds to $\alpha_s = 0.20$. The rate is given by $\frac{\alpha_s}{\pi}\ (1 + \frac{\alpha_s}{\pi})^{-1}\ I$, where I is independent of the energy. Measuring the cross section of these large-angle events leads to an independent determination of α_s and Λ , respectively. This has become a burning issue now, in particular, as the new μ - production data [27) 28)] look rather flat at larger q^2. With higher q^2 being reached soon, it should also be possible to test if the effective coupling constant really runs. From 25 GeV to 40 GeV the rate should decrease by ~ 10 % for the parameters given. This would be the really discriminative test of QCD, while the mere existence of three-jet events can also be attributed to alternate field theories with a small fixed point coupling. Söding in his talk at the EPS conference [29)] has attempted to analyze the TASSO data along the lines discussed here, and they found quite a few three-jet events. For a conclusive analysis one will need, however, O(5000) hadronic events which is somewhat in the future.

The angular distribution of the three-jet events with respect to the beam and beam polarization axis is the next point to be investigated. In this

quarks is the $\sim 1 + \cos^2\theta$ distribution of the jet axis in e^+e^- annihilation first observed at SPEAR [30]. The three-jet cross section displaying the full angular dependence is of the form [31]

$$(2\pi)^2 \frac{d^4\sigma}{d\cos\theta\, d\chi\, d\phi\, dT} = \frac{3}{8}(1+\cos^2\theta + P^+P^-\sin^2\theta\cos 2\phi)\frac{d\sigma_U}{dT}$$
$$+ \frac{3}{4}(1 - P^+P^-\cos 2\phi)\sin^2\theta\,\frac{d\sigma_L}{dT} + \frac{3}{4}\left[(\sin^2\theta + P^+P^-\cos 2\phi(1+\cos^2\theta))\cos 2\chi\right.$$
$$\left. - 2P^+P^-\sin 2\phi\cos\theta\sin 2\chi\right]\frac{d\sigma_T}{dT} - \frac{3}{\sqrt{2}}\left[(1 - P^+P^-\cos 2\phi)\cos\theta\cos\chi\right.$$
$$\left. + P^+P^-\sin 2\phi\sin\chi\right]\sin\theta\,\frac{d\sigma_I}{dT}, \qquad (2.8)$$

where the e^+ (e^-) beam has natural transverse polarization P^+ (P^-). The angle Θ is the angle between the thrust axis, i.e., the direction of the most energetic jet and the beam axis, while χ and ϕ are azimuthal angles as defined in Fig.7. The various cross sections read *) [31]

$$\frac{d\sigma_U}{dT} = \frac{2}{3}\frac{\alpha_s}{\pi}\sigma_0\left[\frac{2(3T^2-3T+2)}{T(1-T)}\ln\frac{2T-1}{1-T} - \frac{3(3T-2)(2-T)}{1-T}\right.$$
$$\left. - \frac{2(8T-3T^2-4)}{T^2}\right],$$
$$\frac{d\sigma_L}{dT} = \frac{2}{3}\frac{\alpha_s}{\pi}\sigma_0\,\frac{2(8T-3T^2-4)}{T^2},$$
$$\frac{d\sigma_T}{dT} = \frac{1}{2}\frac{d\sigma_L}{dT}, \qquad (2.9)$$
$$\frac{d\sigma_I}{dT} = \frac{2}{3}\frac{\alpha_s}{\pi}\sigma_0\sqrt{2}\,(2-2T+T^2)\left[\frac{2}{T^2}\sqrt{2T-1} - \frac{1}{T\sqrt{1-T}}\right].$$

They are drawn in Fig.8. For zero polarization ($P^+ = P^- = 0$) and/or averaged over the azimuthal angle ϕ we obtain the angular distribution of three-jet events

*) Note that $\sigma = \sigma_U + \sigma_L$.

T	$\alpha(T)$	$\beta(T)$	$\gamma(T)$
0.7	0.29	0.18	0.04
0.75	0.44	0.14	0.08
0.8	0.60	0.10	0.10
0.85	0.75	0.06	0.10
0.9	0.87	0.03	0.09

$$1 + \alpha(T)\cos^2\Theta + \beta(T)\sin^2\Theta\cos 2\chi + \gamma(T)\sin 2\Theta\cos\chi \qquad (2.10)$$

The most striking and most easy to measure feature is the rather strong deviation of the thrust axis distribution from $1 + \cos^2\Theta$ as T decreases. The coefficients α and β are related by (cf. Eqs. (2.8) and (2.9))

$$\beta(T) = \frac{1-\alpha(T)}{4} \qquad (2.11)$$

which also constitutes an important test. The distributions for polarized beams can be directly read off from Eqs. (2.8) and (2.10). The extra ϕ dependence will be of great help to determine α, β and γ.

Test of Gluon Spin

In order to get an idea how far the angular distributions give evidence of the vector nature of quantum glue let us consider a model where the quarks are coupled to massless scalar gluons:

$$\mathcal{L}_I = g\,\bar{f}\,\lambda_a\,\phi_a\,f. \qquad (2.12)$$

For zero-mass quarks all results of scalar gluons are identical to those of pseudoscalar gluons because of the γ_5 invariance. We obtain the three-jet cross sections [32]

$$\frac{d\sigma_U}{dT} = \frac{1}{3}\frac{\alpha_s^*}{\pi}\sigma_0\left[2\ln\frac{2T-1}{1-T} + \frac{(4-3T)(3T-2)}{1-T} - \frac{2(3T-2)}{T}\right],$$

$$\frac{d\sigma_L}{dT} = \frac{1}{3}\frac{\alpha_s^*}{\pi}\sigma_0\,\frac{2(3T-2)}{T}, \qquad \frac{d\sigma_T}{dT} = \frac{1}{2}\frac{d\sigma_L}{dT},$$

$$\frac{d\sigma_I}{dT} = \frac{1}{3}\frac{\alpha_s^*}{\pi}\sigma_0\sqrt{2}\left[\frac{2(1-T)\sqrt{2T-1}}{T} - \sqrt{1-T}\right] \qquad (2.13)$$

and the angular distribution

T	$\alpha(T)$	$\beta(T)$	$\gamma(T)$
0.7	0.24	0.19	0.02
0.75	0.30	0.18	0.04
0.8	0.37	0.16	0.05
0.85	0.47	0.13	0.04
0.9	0.58	0.11	0.03

$$1 + \alpha(T)\cos^2\theta + \beta(T)\sin^2\theta\cos 2\chi + \gamma(T)\sin 2\theta\cos\chi \qquad (2.14)$$

The largest difference to the vector case consists in $\alpha(T)$. This is shown in Fig. 9. At maximum the difference is almost a factor two which should be sufficient for ruling out scalar and pseudoscalar gluons.

The question of how to measure the spin of the gluon has been raised also by other authors [33) 34)]. I like to stress, however, that the test proposed here is particularly easy to accomplish. Furthermore, the angular distribution (2.14) is least sensitive to the mass of the scalar/pseudoscalar gluon, and there is no reason why is should be zero.

Higher Twist Contributions

Higher-twist contributions like those shown in Fig. 10 also lead to a three-jet-like final state with one jet being a single pion or a resonance.

They fall off one power higher in q^2 than the point-like cross section. But there is any reason to believe that they will still play a role at PETRA and PEP energies, though their order of magnitude estimate [3)] is not really satisfactory, and I would like to see more work being done along the lines of Brodsky and Lepage [16)]. The characteristic feature of these higher-twist contributions is that the invariant mass of one of the jets is rather low (< 2 GeV) what makes them easy to distinguish from gluon bremsstrahlung events.

Four-Jet Final States

Apart from the fact that the effective coupling constant (1.1) vanishes for $q^2 \to \infty$ and some more indirect indications, QCD shows its full gauge structure only in order α_s^2 or higher where the triple-gluon coupling comes in (cf. Fig. 1c). If we could separate four-jet from three- and two-jet events this would also allow a more precise determination of α_s ($O(\alpha_s^2)$!). Furthermore, four-jet final states would be an excellent place to test if α_s really decreases like $1/\ln q^2$.

The canonical quantity to investigate here is $d\sigma/dA$ which, for not too small A, eliminates the dominant two- and three-jet events. This cross section has been studied numerically in Refs. 35, 36 and partly in Ref. 3. In the leading logarithm approximation it takes the simple form [36)]

$$\frac{d\sigma}{dA} = \frac{8}{9}\left(\frac{\alpha_s}{\pi}\right)^2\sigma_0\,\frac{1}{A}\,|\ln^3 A| \qquad (2.15)$$

which only receives contribution from $q\bar{q}gg$ production, while the cross section for $q\bar{q}q\bar{q}$ production is one power in ln A down. Eq. (2.15) is a fairly good approximation to the exact calculation as can be seen from Fig. 11. The cross section $d\sigma(e^+e^- \to q\bar{q}q\bar{q})/dA$ was found to be ~ 10 times smaller than $d\sigma(e^+e^- \to q\bar{q}qq)/dA$ over most of the A region which

has some interesting consequences. The singularity for $A \to 0$ is due to the infrared singularities associated with soft and collinear emission of gluons, quarks and antiquarks.

In the three-jet case we found that lowest order perturbation theory is (probably) valid up to $T \approx 0.9$. This corresponds to $A \approx 0.05$ in the four-jet case, if phrased in terms of jet angles, and applying the same minimal angles to the four-jet case. Disregarding the two- and three-jet background for the moment which for nonasymptotic energies will also contribute to $A > 0$, we then obtain for the rate at which four-jet events are produced ($\sqrt{q^2} = 40$ GeV)

$$\frac{1}{\sigma_0} \int_{0.05}^{A_{max}} dA \, \frac{d\sigma}{dA} = 5\% \quad , \quad A_{max} = \frac{2}{3} . \tag{2.16}$$

This is a sizable rate but does not imply too much yet. The question is: can we exploit the full perturbative domain? This would mean that four-jet events and nonperturbative background are clearly separated. The answer is yes. But not without further cuts on $d\sigma/dA$ as we will see. The more appropriate quantity to study would be the double differential cross section $d^2\sigma/dTdA$, but unfortunately this has not been calculated yet. The nonperturbative two-jet background to $d\sigma/dA$ has been calculated based on the Feynman-Field model *). This is shown in Fig. 11. We see that in $d\sigma/dA$ perturbation theory will only start to dominate over the non-perturbative background at $A \gtrsim 0.1$ for upper PETRA and PEP energies. On that basis we expect indeed a rather small four-jet signal [5]. With help of a little algebra we find, however,

$$\langle T \rangle \lesssim 1 - \frac{\pi}{4} \sqrt{\langle A \rangle} \tag{2.17}$$

*) The three-jet background is expected to have a similar shape, but to be much smaller.

for four-jet events, while for the nonperturbative two-jet background

$$\langle T \rangle \approx 1 - \frac{\pi}{8} \sqrt{\langle A \rangle} . \tag{2.18}$$

Hence, in (T,A) - space four-jet events and background are well separated as is sketched in Fig. 12. This means, if we restrict our analysis to the hatched region in Fig. 12 we do not loose many four-jet events but most of the background will go away.

Another way of looking at four-jet events is to plot $d\sigma/dT$ with a small acoplanarity cut-off. The QCD prediction for that is drawn in Fig. 13. For smaller values of T the four- and three-jet cross sections are of the same order of magnitude, while for *) $1/\sqrt{3} \leq T \leq 2/3$ only four-jet events (and higher) contribute to $d\sigma/dT$. This means for $T < 0.8$ we should see a fair number of jet events with a rather fat jet (i.e, two unresolved jets) in either hemisphere, whereas three-jet events are expected to consist of a fat and a narrow jet [25].

From Fig. 13 we gather that four-jet events also constitute a non-negligible background to the three-jet cross section (2.1), in particular for smaller T. This is to say that Eq. (2.1) should only be used in connection with an acoplanarity cut-off. The "gold-plated" QCD test discussed earlier is, however, not affected.

Let us now go back to Fig. 11. We have seen that four-jet events consist to ~ 90 % of $q\bar{q}gg$ final states. So the hatched region in Fig. 12 is the ideal place where to study the particulars of gluon jets in the continuum ("gluon factory"). One should watch out for fast neutrals (η , η') and a

*) The kinematical boundaries for three- and four-jet events are $T \geq 2/3$ and $T \geq 1/\sqrt{3}$, respectively.

possibly higher multiplicity [37]. Because gluons are flavour blind we also expect an excess of, e.g., fast K^0, $\bar{K}^0$ in this region.

The Three-Gluon Vertex

Four-jet events will typically consist of three distinctive jets with one jet being evidently fatter than the others. Since *) [14) 20) 21)]

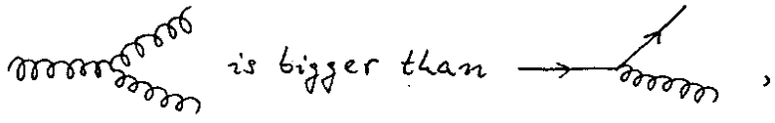

we expect, viewed from the parent three-jet level, that the fat jet will mostly be the gluon jet rather than the quark or antiquark jet **). For an abelian vector theory, on the other hand, the opposite will be true. That is, here we expect the fat jet to be dominantly the quark or antiquark jet. Supposing that one knows how to distinguish quark and gluon jets, this will be a nice and feasible test of the nonabelian gauge structure of the theory.

The absolute value of the four-jet cross section will be a further check on the three-gluon coupling, provided one knows already the effective coupling constant (which can be obtained from the three-jet cross section). The effect the gauge group has on the magnitude of the four-jet cross section is illustrated by ***)

$$\sigma_{QCD}(e^+e^- \to q\bar{q}gg)/\sigma_{3C}(e^+e^- \to q\bar{q}gg) = 2.2, \quad A \geq 0.05 \tag{2.19}$$

*) The gluon branching into $q\bar{q}$ is negligible here, as we have seen.

**) If quark and antiquark jets are not distinguished, one looses a factor two though.

where σ_{3C} (3C standing for three-colour model [38]) is three times the QED cross section ($\alpha = \alpha_s$).

Heavy Flavour Production

For the associated production of heavy $Q\bar{Q}$ pairs,

$$e^+e^- \to Q\bar{Q}Q\bar{Q}, \tag{2.20}$$

there is no need for a cut-off since the heavy quark masses provide a natural infrared cut-off. Hence, $\sigma(e^+e^- \to Q\bar{Q}Q\bar{Q})$ can be calculated perturbatively (Fig. 14). Taking m_c = 1.6 GeV and m_b = 4.6 GeV we obtain [36) 39)] (relative to $Q\bar{Q}$ production)

$\sqrt{q^2}$ (GeV)	R ($\frac{c\bar{c}c\bar{c}}{c\bar{c}}$)	R ($\frac{c\bar{c}b\bar{b}}{b\bar{b}}$)	R ($\frac{b\bar{b}b\bar{b}}{b\bar{b}}$)
40	0.0043	0.0049	0.00024
80	0.0091	0.016	0.0016

(2.21)

This is to be interpreted as the total inclusive $c\bar{c}c\bar{c}$, etc. production cross section, i.e.,

$$\sigma(e^+e^- \to \left\{ \begin{matrix} \psi+\psi \\ \psi+D\bar{D} \\ \vdots \end{matrix} \right\} + X), \text{ etc.} \tag{2.22}$$

The rate is on the level of half a % at the upper PETRA and PEP energies which is not exactly very high. It should, however, be stressed that this is a rather clean prediction as it does not require to impose any infrared cutoff on the data. Moreover, it is practically free of any sizable background.

3. Hadron Distributions in Jets and Correlations

The hadron distribution in e^+e^- jets bears the same information on the dynamics at short distances (and more) as is mediated by the perturbative jet measures discussed in the last section. For instance will the secondary hadrons retain the direction of their parent quark, antiquark or gluon up to a finite, nonperturbative $\langle p_T \rangle_{NP} = 0$ (300 MeV) which at high enough energies can be neglected. That this involves the gluon fragmentation function as an unknown (the quark fragmentation functions are, in principle, known from lower energies) is rather a positive feature as it will answer such important questions as: is the gluon flavour blind?

Single-Hadron Distribution

The semi-inclusive e^+e^- annihilation cross section is given by *)

$$\frac{d^2\sigma}{d\cos\theta\, dx} = \frac{3}{8}(1+\cos^2\theta)\frac{d\sigma_U}{dx} + \frac{3}{4}\sin^2\theta\,\frac{d\sigma_L}{dx}\,, \qquad (3.1)$$

where θ now is the angle between the hadron momentum and the beam axis. In the naive quark-parton model (zeroth order QCD)

$$\frac{d\sigma_L}{dx} \approx 2\,\frac{\langle p_T^2\rangle_{NP}}{q^2 x^2}\,\frac{d\sigma}{dx} \xrightarrow[q^2\to\infty]{} 0 \qquad (3.2)$$

which asymptotically leads to a $1 + \cos^2\theta$ angular distribution. A non-vanishing σ_L arises if $\langle p_T^2 \rangle \sim q^2$ (within logarithms). This is expected in first (and higher) order in α_s as a result of hard gluon bremsstrahlung.

*) Experimentalists often use "σ_T" and "σ_L": "σ_T" = σ_U and "σ_L" = 2 σ_L. The cross section for polarized beams can be read off from (2.8).

Neglecting the nonperturbative p_T (i.e., for large q^2) we find *) 40)

$$\frac{d\sigma_L}{dx} = \int_x^1 \frac{dx_q}{x_q}\,\frac{d\sigma_L}{dx_q}\,\mathcal{D}_q\!\left(\frac{x}{x_q}\right) + \int_x^1 \frac{dx_{\bar q}}{x_{\bar q}}\,\frac{d\sigma_L}{dx_{\bar q}}\,\mathcal{D}_{\bar q}\!\left(\frac{x}{x_{\bar q}}\right) + \int_x^1 \frac{dx_g}{x_g}\,\frac{d\sigma_L}{dx_g}\,\mathcal{D}_g\!\left(\frac{x}{x_g}\right), \qquad (3.3)$$

$$\frac{d\sigma_L}{dx_q} = \frac{d\sigma_L}{dx_{\bar q}} = \frac{2}{3}\frac{\alpha_s}{\pi}\sigma_0\,, \quad \frac{d\sigma_L}{dx_g} = \frac{2}{3}\frac{\alpha_s}{\pi}\sigma_0\,\frac{4(1-x_g)}{x_g}\,,$$

where $x_i = 2p_i/\sqrt{q^2}$, $i = q, \bar q, g$. It should be noted that (to order α_s) σ_L is infrared finite. Writing

$$\frac{d^2\sigma}{d\cos\theta\, dx} = (1+\alpha(x)\cos^2\theta)\,\frac{1}{2+\frac{2}{3}\alpha(x)}\,\frac{d\sigma}{dx}\,, \qquad (3.4)$$

this gives

$$\alpha(x) = 1 - 4\,\frac{d\sigma_L/dx}{d\sigma/dx + d\sigma_L/dx}\,. \qquad (3.5)$$

I have plotted $\alpha(x)$ in Fig. 15 for fragmentation functions **)

$$\mathcal{D}_q^c(x) = \mathcal{D}_{\bar q}^c(x) = 2\,\frac{(1-x)^2}{x} \qquad (3.6)$$

and

*) We have omitted the q^2-dependence from the argument of the fragmentation functions.

**) Being in agreement with the counting rules [16].

$$A: \quad D_g^c(x) = \int_x^1 \frac{dx_f}{x_f} D_f^c\left(\frac{x}{x_f}\right) + \int_x^1 \frac{dx_{\bar f}}{x_{\bar f}} D_{\bar f}^c\left(\frac{x}{x_{\bar f}}\right)$$

$$= 4\,\frac{1-x^2}{x} + 8 \ln x \,, \qquad (3.7)$$

$$B: \quad D_g^c(x) = D_f^c(x) = 2\,\frac{(1-x)^2}{x} \,, \qquad (3.8)$$

where c stands for the sum over all charged particles. Choice A corresponds to the case where the gluon fragments first into a quark and antiquark, respectively, with a flat momentum distribution [41] which then decay with fragmentation function (3.6). Choice A is somewhat softer than choice B. Also shown is the nonperturbative background. For smaller x we find a sizable (and lasting as q^2 increases) deviation of $\alpha(x)$ from 1 which is much bigger than what we expect from the nonperturbative background. The difference between A and B is not significant.

Transverse Momentum Profile of e^+e^- Jets

Let me recall that for $q\bar{q}g$ final states the thrust axis is parallel to the direction of the most energetic jet which makes it the canonical axis for studying p_T phenomena. The hadron transverse momentum with respect to the thrust axis is given by the transverse momentum of the recoiling partons smeared with the fragmentation functions [42] (Fig. 16):

$$\frac{1}{\sigma}\frac{d^2\sigma}{dx\,d p_T^2} = \frac{1}{6}\frac{\alpha_s}{\pi}\,\frac{1}{p_T^2}\,\frac{1-\varkappa^2}{\varkappa}\int_x^{\frac{2-\sqrt{2}(1-\varkappa)}{1+\varkappa}} dz\,\frac{1}{1-z}\,A^2$$

$$\times\left[\left(\frac{A^2+z^2}{3(1-z)} + \frac{(1-z+3)^2+z^2}{(z-3)(1-z)}\right)\left(D_f\left(\frac{x}{z}\right)+D_{\bar f}\left(\frac{x}{z}\right)\right) + 2\,\frac{A^2+(1-z+3)^2}{3(z-3)}\,D_g\left(\frac{x}{z}\right)\right],$$

$$\varkappa = \sqrt{1-p_T^2/p^2} = \sqrt{1-x_T^2/x^2}\,, \qquad x_T = 2p_T/\sqrt{q^2}\,,$$

$$z(1-3) \qquad\qquad z(1-\varkappa)$$

where the nonperturbative p_T relative to the parent parton has been neglected. For $p_T^2 \to 0$ and $q^2 \to \infty$, p_T fixed Eq. (3.9) reduces to

$$\frac{1}{\sigma}\frac{d^2\sigma}{dx\,d p_T^2} \approx \frac{2}{3}\frac{\alpha_s}{\pi}\,\frac{|\ln p_T/x\sqrt{q^2}|}{p_T^2}\left(D_f(x)+D_{\bar f}(x)\right), \qquad (3.10)$$

and it is obviously not applicable where the logarithm becomes large.

Equation (3.9) has some interesting qualitative features. Disregarding the q^2-dependence of the fragmentation functions, it leads to the scaling laws

$$\frac{1}{\sigma}\frac{d^2\sigma}{dx\,d p_T^2} = \frac{\alpha_s(q^2)}{p_T^2}\,f(x,x_T)\,,$$

$$\frac{1}{\sigma}\frac{d^2\sigma}{dx\,dx_T} = \alpha_s(q^2)\,g(x,x_T)\,, \qquad (3.11)$$

$$\frac{1}{\sigma}\frac{d\sigma}{d p_T^2} = \frac{\alpha_s(q^2)}{p_T^2}\,f(x_T)\,.$$

These are to be compared to

$$\frac{1}{\sigma}\frac{d^2\sigma}{dx\,d p_T^2} = \frac{c}{p_T^4}\,h(x,x_T) \qquad (3.12)$$

(c has dimension $(\text{mass})^2$) for the higher-twist contributions in Fig. 10 and an exponential decrease of the nonperturbative jet spread. I find it very important to establish the $1/p_T^2$ fall-off for fixed x, x_T which really will tell how much of the jet broadening is due to gluon bremsstrahlung and how much to higher-twist contributions and nonperturbative background. This requires, of course, to compare data at different q^2.

There is data only for $d\sigma/d p_T^2$ from TASSO [43]. This as well as the QCD prediction [42] is shown in Fig. 17. We find good agreement with the data if the (nonperturbative) zeroth order contribution is taken into account

But I would like to see more data at higher p_T where the low-x region, which is always good for surprises and where one runs into infrared problems (cf. Eq. (3.10)), is turned off as one can see from Fig. 18.

Hard gluon bremsstrahlung will, likewise, be reflected in the average transverse momentum of hadrons:

$$\langle p_T^2(x)\rangle = \int d p_T^2\, p_T^2\, \frac{1}{\sigma}\frac{d^2\sigma}{dx\, dp_T^2} \Big/ \frac{1}{\sigma}\frac{d\sigma}{dx} \,. \qquad (3.13)$$

Unlike $d\sigma/dp_T^2$ at very large p_T, this also includes the nonperturbative background and other possible contributions. But for large q^2 and medium x we expect (3.13) to be largely determined by single gluon bremsstrahlung, which unmistakably grows like [12)40)]

$$\langle p_T^2(x)\rangle \sim \alpha_s(q^2)\, q^2 \,. \qquad (3.14)$$

In Fig. 19 I have shown the QCD prediction (i.e., (3.9) inserted into (3.13)) together with the TASSO data [29)]. Both, theoretical and experimental curves show a more or less distinct "seagull" structure [40)], and as far as one can tell, there is good agreement at the highest energy *). At lower energies and small x the perturbation calculation is not supposed to give the correct average transverse momentum. But the trend of the data is very much in favour of a rising $\langle p_T^2(x)\rangle$ à la (3.14).

*) Only shown is the QCD prediction for the gluon fragmentation function (3.8) which gives a slightly better fit.

Several authors have written Monte Carlo programs as to include the nonperturbative jet broadening. But for quantities like $\langle p_T^2(x)\rangle$ this does not present much of an improvement since at high q^2 perturbation theory breaks down (cf. Eq. (3.10)) long before p_T reaches 300 MeV (i.e., the nonperturbative average transverse momentum). The real improvement, I think, would be to include multigluon bremsstrahlung (jet branching).

A further implication of hard gluon bremsstrahlung is a strong asymmetry in the transverse momentum distribution. That is, we expect one broad and one narrow jet. This idea has been pursued by the authors of Ref. 25. Their prediction as well as the data is shown in Fig. 20. There is agreement also here.

Two-Particle Correlations (kinematic)

In the naive quark-parton model the back-to-back jets factorize if the sum is taken over, e.g., all charged particles. That is *)

$$\left(\frac{1}{\sigma}\frac{d^2\sigma^{cc}}{dx_1\, dx_2}\right)_{\substack{\text{opposite}\\ \text{hemisphere}}} = \frac{1}{2}\,\frac{1}{\sigma}\frac{d\sigma^c}{dx_1}\,\frac{1}{\sigma}\frac{d\sigma^c}{dx_2} \qquad (3.15)$$

*) The left-hand-side of (3.15) is the cross section for finding a charged hadron with fractional momentum x_1 in either one jet and a charged hadron with momentum x_2 in the respective opposite jet.

for a single flavour or for identical fragmentation functions $D_{q_f}^c$ (= $D_{\bar{q}_f}^c$), f = u,d,s,... . The latter is expected for large q^2. In case the fragmentation functions are different Eq. (3.15) reduces to *)

$$\int_0^1 dx_2\, x_2 \left(\frac{1}{\sigma}\frac{d^2\sigma^{cc}}{dx_1\,dx_2}\right)_{\substack{\text{opposite}\\ \text{hemisphere}}} = \frac{2}{3}\,\frac{1}{\sigma}\,\frac{d\sigma^c}{dx_1}\,. \qquad (3.16)$$

This means essentially that there is no energy correlation between the two hemispheres.

Not so in QCD. Here we expect an energy asymmetry like the asymmetry in the transverse momentum. Let us define the correlation function [45]

$$C^{cc}(x_1,x_2) = \left(\frac{1}{\sigma}\frac{d^2\sigma^{cc}}{dx_1 dx_2}\right)_{\substack{\text{opposite}\\ \text{hemisphere}}} - \frac{1}{2}\,\frac{1}{\sigma}\frac{d\sigma^c}{dx_1}\,\frac{1}{\sigma}\frac{d\sigma^c}{dx_2}\,. \qquad (3.17)$$

In QCD this does not vanish, contrary to Eq. (3.15). It is interesting to note that $C^{cc}(x_1,x_2)$ is explicitly infrared finite (in the limit of large q^2) which saves us the infrared "renormalization". In Fig. 21 I have shown

$$C^{cc}(x_1,x_2) \,/\, \mathcal{D}_f^c(x_1)\,\mathcal{D}_{\bar{f}}^c(x_2) \qquad (3.18)$$

for the fragmentation functions (3.6) - (3.8) ($D_q^c = D_u^c = D_d^c = \ldots$). The

*) Here we have assumed $\int_0^1 dx\, x\, \mathcal{D}_{q_f}^c(x) = \frac{1}{3}$.

predicted correlation is quite large. For medium x_1, x_2 , where we can count upon sufficient statistics, (3.18) is of the order of 20 %.

For nonasymptotic q^2, where quark masses cannot be neglected, the light and heavy quark fragmentation functions will generally be different. In this case a nonvanishing $C^{cc}(x_1,x_2)$ is not confidently a signature of QCD. But we obtain in zeroth order (Q_q, Q_Q are the light and heavy quark charges, respectively)

$$C^{cc}(x_1,x_2) = \frac{2\,Q_f^2\,Q_Q^2}{(Q_f^2+Q_Q^2)^2}\left(\mathcal{D}_f^c(x_1)-\mathcal{D}_Q^c(x_1)\right)\left(\mathcal{D}_{\bar{f}}^c(x_2)-\mathcal{D}_{\bar{Q}}^c(x_2)\right) \qquad (3.19)$$

and similarly for the more realistic case of several light and heavy quarks. Only for q^2 far above $4m_Q^2$ can we expect (3.20) to vanish. The contribution (3.19) is, however, rather small. If we allow D_q^c and D_Q^c to differ by 20 % this gives a 2 % (1.3 %) correction to (3.18) for equal (different) quark charges which is to be compared to, say, a 20 % QCD effect.

The non-QCD background can be fully eliminated by integrating over the energy in the jet, e.g., opposite to particle 1, i.e.,

$$\int_0^1 dx_2\, x_2\; C^{cc}(x_1,x_2) = O(\alpha_s)\,, \qquad (3.20)$$

which constitutes a genuine signal of QCD now. In Fig. 22 I have shown

$$\int_0^1 dx_2\, x_2\; C^{cc}(x_1,x_2) \,/\, \mathcal{D}_f^c(x_1)\,. \qquad (3.21)$$

A somewhat diminished signal (as compared to (3.18)) is the price one has to pay for having eliminated the background completely.

Taking the energy weighted average over both jets brings us close to the energy correlations considered by the Seattle group [46]. That is

$$\left(\langle E_1^c E_2^c\rangle_{\substack{\text{opposite}\\ \text{hemisphere}}} - \tfrac{1}{2}\langle E_1^c\rangle\langle E_2^c\rangle\right)\left(\tfrac{1}{2}\langle E_1^c\rangle\langle E_2^c\rangle\right)^{-1}$$

$$= \int_0^1 dx_1 x_1 \int_0^1 dx_2 x_2\, C^{cc}(x_1,x_2)\left(\tfrac{1}{2}\int_0^1 dx_1 x_1 \tfrac{1}{\sigma}\tfrac{d\sigma^c}{dx_1}\int_0^1 dx_2 x_2 \tfrac{1}{\sigma}\tfrac{d\sigma^c}{dx_2}\right)^{-1}$$

$$= -0.10\ \frac{\alpha_s}{\pi} \qquad (3.22)$$

This has the advantage of not depending anymore on the fragmentation functions. But, in contrast to (3.18) and (3.21), the effect (over the background) is rather small and has probably no chance to be measured.

Charge Correlations

In the applications discussed so far the fact that the gluon is flavour neutral was only implicitly made use of. As a more direct test of (in the first place) the charge of the gluon it is important to search for charge correlations between hadrons in different jets, i.e., at large angles.

In quark (antiquark) jets the parent quark (antiquark)is most likely carried by the high momentum leading hadron, while gluon jets, on the other hand, should not show any charge asymmetry at any x. This gives

us a handle to identify the charge of the parent parton. We also expect the total charge of all the fragments in a jet, averaged over many events, to be equal to the charge of the parent quark, antiquark or gluon up to an universal (but energy dependent) constant [47].

Let us first consider the leading particle charge correlations. The quantity to be discussed here is the two-particle inclusive cross section *)

$$\frac{d^3\sigma^{h_1 h_2}}{dx_1\, dx_2\, d\cos\vartheta}\ , \qquad (3.23)$$

where ϑ is the angle between the momenta of hadron h_1 and h_2 (Fig. 23). For u quarks the ratio of fragmentation functions into negatively and positively charged hadrons was found to be **) [48]

$$D_u^-(x)\,/\,D_u^+(x) = \frac{1-x}{1+x}\ . \qquad (3.24)$$

The same/similar is expected for the other quarks:

$$Q_q = \tfrac{2}{3}\ :\ D_q^-(x)\,/\,D_q^+(x) = \frac{1-x}{1+x}\ ,$$
$$Q_q = -\tfrac{1}{3}\ :\ D_q^+(x)\,/\,D_q^-(x) = \frac{1-x}{1+x}\ , \qquad (3.25)$$

*) This is explicitly infrared finite to order α_s for $0^\circ < \vartheta < 180^\circ$.

**) $D_u^-(x) = D_{\bar u}^+(x)$.

whereas

$$D_g^+(x) = D_g^-(x). \tag{3.26}$$

For $\cos\vartheta \to -1$ the cross section (3.23) reduces to

$$\frac{d^3\sigma^{h_1,h_2}}{dx_1\,dx_2\,d\cos\vartheta} \sim D_g^{h_1}(x_1)\,D_{\bar{g}}^{h_2}(x_2) + D_{\bar{g}}^{h_1}(x_1)\,D_g^{h_2}(x_2) \tag{3.27}$$

and thus connects smoothly to the naive quark-parton model result

$$d\sigma^{++}/d\sigma^{+-} \to 0 \quad \text{for } x_{1,2} \to 1. \tag{3.28}$$

For three-jet events and $|\cos\vartheta| < 1$, on the other hand, we expect

$$d\sigma^{++}/d\sigma^{+-} \to \text{const.}\ (\neq 0) \quad \text{for } x_{1,2} \to x_{1,2}^{max} \tag{3.29}$$

due to the emission of hard flavourless gluons. In Fig. 24 I have shown [49] $d\sigma^{++}/d\sigma^{+-}$ for fragmentation functions (3.6), (3.8) for $x_1 \leq 0.8$ and x_2/x_2^{max} fixed *) as a function of $\cos\vartheta$. The effect is significant though the cross section is fairly small in this region. In order to increase statistics it is advisable to consider moments of (3.23) instead.

A different way of testing if the gluon is flavour neutral is to look at the charge flow in three-jet events. Therefore we define the charge-flow

*) $x_2^{max} = 1$ for $\vartheta = 180^0$ and gradually decreases to $x_2^{max} = 0.5$ for $\vartheta = 120^0$.

tensor by

$$Q_{\alpha\beta} = \sum_{i,j}{}' Q_i\,Q_j\,e_\alpha^i\,e_\beta^j\,, \qquad \{i\} \cap \{j\} = 0 \tag{3.30}$$

where, as before, the event is divided into two hemispheres $\{i\}$ and $\{j\}$, respectively. The sum goes over all particles with energy $E_i \geq \epsilon\sqrt{s^2}$ for some fixed ϵ . The $\vec{e}^{\,i}$ are unit vectors pointing into the direction of the i-th hadron. As the reader can easily verify himself and I have no room to explain here in more detail, $Q_{\alpha\beta}$ is infrared insensitive and so its distributions can be calculated in QCD perturbation theory. Implicitly, $Q_{\alpha\beta}$ involves a charge weighting in effectively the same way as introduced in Ref. 50 since the slower particles will be (more or less) randomly distributed. In the presence of hard (flavourless) gluon bremsstrahlung we expect $Q_{\alpha\beta}$ to be systematically non-symmetric while for $q\bar{q}$ initiated final states it should be symmetric. The anti-symmetric part of $Q_{\alpha\beta}$ defines

$$Q_\sigma = \epsilon_{\sigma\alpha\beta}\,Q_{\alpha\beta}\,. \tag{3.31}$$

For three-jet events the vector $\vec{Q}$ is normal to the event plane. Two-jet events, on the other hand, have zero $Q = |\vec{Q}|$.

Let us consider Q now. I have calculated $Q(T) = \langle Q \rangle_T$ (i.e., the average Q for fixed thrust values) for u,d,s and c quarks to order α_s . Note that the low-energy cut-off is ineffective here. This is shown in Fig. 25. The characteristic feature is that $Q(T)$ increases as T decreases.

4. Summary

We have seen that e^+e^- annihilation into hadrons offers truly incisive tests of QCD. I have restricted myself to PETRA and PEP energies. If the $t\bar{t}$ bound states (toponium) should lie as low as $\lesssim$ 38 GeV further tests will come from the 1^{--}, etc. onium decays [5)41)51)-53)].

There is experimental evidence for three-jet events and jet broadening. But much higher statistics and a great deal of experimental work is required to provide bona fide tests of the theory.

Acknowledgement

Part of these notes have been written while I was a visitor at SLAC, and I would like to thank the SLAC theory group for their warm hospitality. I am also indebted to J.D. Bjorken for helpful criticism and discussions. Some of the material presented here draws from unpublished work in collaboration with G. Kramer, J. Willrodt and K. Mursula which is gratefully acknowledged.

References

1. D.J. Gross and F.A. Wilczek, Phys. Rev. D8, 3633 (1973) and D9, 980 (1974); H. Georgi and H.D. Politzer, Phys. Rev. D9, 416 (1974)

2. J. Ellis, M.K. Gaillard and G.G. Ross, Nucl. Phys. B111, 253 (1976)

3. T.A. DeGrand, Y.J. Ng and S.-H.H. Tye, Phys. Rev. D16, 3251 (1977)

4. G. Sterman and S. Weinberg, Phys. Rev. Letters 39, 1436 (1977)

5. A. De Rujula, J. Ellis, E.G. Floratos and M.K. Gaillard, Nucl. Phys. B138, 387 (1978)

6. H.D. Politzer, Phys. Letters 70B, 430 (1977); R.K. Ellis, H. Georgi, M. Machacek, H.D. Politzer and G. Ross, Nucl. Phys. B152, 285 (1979); D. Amati, R. Petronzio and G. Veneziano, Nucl. Phys. B140, 54 (1978) and B146, 29 (1978)

7. H.D. Politzer, Nucl. Phys. B129, 301 (1977), C.T. Sachrajda, Phys. Letters 73B, 185 (1978)

8. Yu. L. Dokshitzer, D.I. D'Yakonov and S.I. Troyan, Proceedings of XIII Winter School of LNPI, Leningrad (1978), Vol. I (English translation: SLAC-TRANS-183 (1978)), and references therein

9. R. Baier and K. Fey, Bielefeld preprint BI-TP 79/11 (1979)

10. R.M. Barnett, invited talk given at the SLAC Summer Institute, Topical Conference, 18-20 July, 1979 (these proceedings)

11. J. Ranft and G. Ranft, Phys. Letters 82B, 129 (1979); P. Binétruy and G. Girardi, Nucl. Phys. B155, 150 (1979); Ch. Rumpf and G. Kramer, DESY preprint DESY 79/62 (1979)

12. H.D. Politzer, Phys. Letters 70B, 430 (1977)

13. R.P. Feynman, Photon-Hadron Interactions, Benjamin (New York, 1972); J.D. Bjorken and E.A. Paschos, Phys. Rev. 158, 1975 (1969); S.D. Drell, D.J. Levy and T.-M. Yan, Phys. Rev. D1, 1617 (1970)

14. A.V. Smilga and M.I. Vysotsky, Nucl. Phys. B150, 173 (1979)

15. E. Farhi, Phys. Rev. Letters 39, 1587 (1977)

16. S.J. Brodsky and G.R. Farrar, Phys. Rev. Letters 31, 1153 (1973); S.J. Brodsky and G.P. Lepage, SLAC preprint SLAC-PUB-2294 (1979)

17. Ref. 3; these authors call it CIM process

18. C.L. Basham, L.S. Brown, S.D. Ellis and S.T. Love, Phys. Rev. D17, 2298 (1978) and D19, 2018 (1979)

19. G. Curci and M. Greco, Phys. Letters 79B, 406 (1978)

20. M.B. Einhorn and B.G. Weeks, Nucl. Phys. B146, 445 (1978)

21. K. Shizuya and S.-H.H. Tye, Fermilab preprint FERMILAB-Pub-79/16-THY (1979)

22. R.K. Ellis and R. Petronzio, Phys. Letters 80B, 249 (1979)

23. K. Konishi, A. Ukawa and G. Veneziano, Phys. Letters 80B, 259 (1979)

24. W. Furmanski, CERN preprint TH.2664-CERN

25. P. Hoyer, P. Osland, H.G. Sander, T.F. Walsh and P.M. Zerwas, DESY preprint DESY 79/21 (1979)

26. A. Ali, J.G. Körner, G. Kramer and J. Willrodt, Zeitschr. f. Physik C1, 203 (1979)

27. V. Korbel, invited talk given at the SLAC Summer Institute, Topical Conference, 18-20 July, 1979 (these proceedings)

28. M. Mugge, invited talk given at the SLAC Summer Institute, Topical Conference, 18-20 July, 1979 (these proceedings)

29. P. Söding, invited talk given at the EPS International Conference on High Energy Physics, Geneva, 27 June - 4 July, 1979

30. G. Hanson et al., Phys. Rev. Letters 35, 1609 (1975)

31. G. Kramer, G. Schierholz and J. Willrodt, Phys. Letters 78B, 249 (1978), erratum ibid. 80B, 433 (1979)

32. G. Kramer and G. Schierholz, unpublished; G. Schierholz, invited talk given at the Nordic Particle Physics Meeting, Copenhagen, 23-25 April, 1979; see also Ref. 25

33. J. Ellis and I. Karliner, Nucl. Phys. B148, 141 (1979)

34. C.L. Basham and S.T. Love, Phys. Rev. D20, 340 (1979)

35. A. Ali, J.G. Körner, Z. Kunszt, J. Willrodt, G. Kramer, G. Schierholz and E. Pietarinen, Phys. Letters 82B, 285 (1979)

36. A. Ali, J.G. Körner, Z. Kunszt, E. Pietarinen, G. Kramer, G. Schierholz and J. Willrodt, DESY preprint DESY 79/54 (1979)

37. K. Konishi, A. Ukawa and G. Veneziano, Phys. Letters 78B, 243 (1978)

38. M. Glück and E. Reya, Phys. Letters 69B, 77 (1977)

39. G.C. Branco, H.P. Nilles and K.H. Streng, Aachen preprint PITHA 79/09 (1979)

40. G. Kramer and G. Schierholz, Phys. Letters 82B, 108 (1979)

41. S.J. Brodsky, D.G. Coyne, T.A. DeGrand andR.R. Horgan, Phys. Letters 73B, 203 (1978); K. Koller and T.F. Walsh, Phys. Letters 72B, 227 (1977)

42. G. Schierholz and J. Willrodt, unpublished

43. R. Brandelik et al., Phys. Letters 86B, 243 (1979)

44. Ch. Berger et al., DESY preprint DESY 79/57 (1979)

45. G. Schierholz and J. Willrodt, DESY preprint DESY 79/32 (1979), to be published in Zeitschr. f. Physik C

46. C.L. Basham, L.S. Brown, S.D. Ellis and S.T. Love, Phys. Rev. D19, 2018 (1979)

47. S.J. Brodsky and N. Weiss, Phys. Rev. D16, 2325 (1977)

48. L.M. Sehgal, in Proceedings of the 1977 International Symposium on Lepton and Photon Interactions at High Energies, Hamburg (ed. F. Gutbrod), p. 837

49. K. Mursula and G. Schierholz, unpublished

50. L. Susskind, in Proceedings of the 1977 International Symposium on Lepton and Photon Interactions at High Energies, Hamburg (ed. F. Gutbrod), p. 895

51. H. Fritzsch and K.H. Streng, Phys. Letters 74B, 90 (1978)

52. M. Krammer and H. Krasemann, Phys. Letters 73B, 58 (1978)

53. K. Koller, H. Krasemann and T.F. Walsh, Zeitschr. f. Physik C1, 71 (1979)

Figure Captions

Fig. 1 Electron-positron annihilation into (a) two-jet, (b) three-jet and (c) four-jet hadronic final states.

Fig. 2 Thrust distribution for $e^+e^- \to q\bar{q}g$ (dashed line) and summed over leading logarithms (dotted line). The solid curve is an eyeball interpolation between (2.1) at low thrust and (2.3) at higher values of T. Here and in the following curves the parameters are $\Lambda = 0.5$ GeV, $N_f = 5$.

Fig. 3 Thrust distribution for $e^+e^- \to q\bar{q}g$ (full line) compared to the light and heavy quark background.

Fig. 4 "Typical" three-jet events for various T. The numbers attached to the jets correspond to their energies.

Fig. 5 Dalitz plot for three-jet events. If we choose Θ_1 (Θ_2) to be the maximal (minimal) jet angle only the lower left triangle will be occupied. The all-large-angle triangle shown (dashed borderlines) corresponds to $\vartheta \leq 140^\circ$, $\vartheta^* \geq 80^\circ$.

Fig. 6 The cross section $\sigma^{-1} d^2\sigma / d\vartheta\, d\vartheta^*$ on the borderlines of the Dalitz plot. Left-hand side: $\vartheta^* = 360^\circ - 2\vartheta$. Right-hand side: $\vartheta = 360^\circ - 2\vartheta^*$.

Fig. 7 Definition of Euler angles Θ, χ and ϕ. The event lies in the (x,z) plane. The thrust axis is along $\vec{Oz}$, and $\vec{Ox}$ points into the direction of the second most energetic jet. Θ, χ and ϕ vary between $0 \leq \Theta \leq \pi$, $0 \leq \chi \leq 2\pi$ and $0 \leq \phi \leq 2\pi$.

Fig. 8 Partial cross sections. U: $d\sigma_U/dT$, L: $d\sigma_L/dT$ and I: $d\sigma_I/dT$; $d\sigma_T/dT = \frac{1}{2} d\sigma_L/dT$.

Fig. 9 Angular coefficient of thrust axis distribution $(\sim 1+\alpha(T)\cos^2\Theta)$ versus T for vector and scalar/pseudoscalar gluons.

Fig. 10 Higher-twist contributions to e^+e^- annihilation into hadrons.

Fig. 11 The cross section $\sigma^{-1} d\sigma/dA$ for $e^+e^- \to q\bar{q}gg$ (full curve), $e^+e^- \to q\bar{q}q\bar{q}$ (dashed curve) and in the leading logarithm approximation (dashed-dotted curve). The dashed-twice-dotted curve is the nonperturbative two-jet background.

Fig. 12 Regions of phase space for some finite energy. The hatched region is where we expect four-jet events. The dotted area will be populated by the two- and three-jet "background".

Fig. 13 Thrust distribution with acoplanarity cut-off $A \geq 0.05$ for $e^+e^- \to q\bar{q}gg + q\bar{q}q\bar{q}$. Also drawn is the thrust distribution for $e^+e^- \to q\bar{q}g$ for comparison.

Fig. 14 Heavy $Q\bar{Q}Q\bar{Q}$ production diagrams.

Fig. 15 Angular coefficient of semi-inclusive hadron distribution $(\sim 1+\alpha(x)\cos^2\Theta)$ for gluon fragmentation functions A and B (full curve). The dashed curve corresponds to the non-perturbative two-jet contribution $\alpha(x) = 1 - 8\langle p_T^2\rangle_{NP}/x^2 Q^2$; $\langle p_T^2\rangle_{NP} = (300\ \mathrm{MeV})^2$.

Fig. 16 Dynamics of jet broadening. The dashed line corresponds to the thrust axis.

Fig. 17 Transverse momentum distribution. The data is from Ref. 43 and measures p_T with respect to the sphericity axis. The curve is our prediction for $\sqrt{q^2}$ = 30 GeV and gluon fragmentation function B.

Fig. 18 Double differential cross section $d^2\sigma/dx\,dp_T^2$ for various values of x and gluon fragmentation function B.

Fig. 19 The average transverse momentum of hadrons versus x. The data is from Ref. 29.

Fig. 20 The asymmetry in $\langle p_T^2(x)\rangle$. The data is from PLUTO [44]. There is also TASSO data [43] which lies systematically lower but shows the same effect.

Fig. 21 The (normalized) correlation function (3.18) for (a) gluon fragmentation function A and (b) gluon fragmentation function B. One block corresponds to $x_{1,2} = 0.1$. The triangle $x_2 > x_1$, which is symmetric to $x_1 > x_2$, has been cut away for better view.

Fig. 22 The energy integrated (normalized) correlation function (3.21) for gluon fragmentation functions A and B.

Fig. 23 Kinematics of two-particle inclusive cross section.

Fig. 24 The ratio $d\sigma^{++}/d\sigma^{+-}$ for $x_1 \gtrsim 0.8$ and $x_2/x_2^{max} = 0.4$ and $x_2/x_2^{max} = 0.6$, respectively.

Fig. 25 $Q(T)$ versus T.

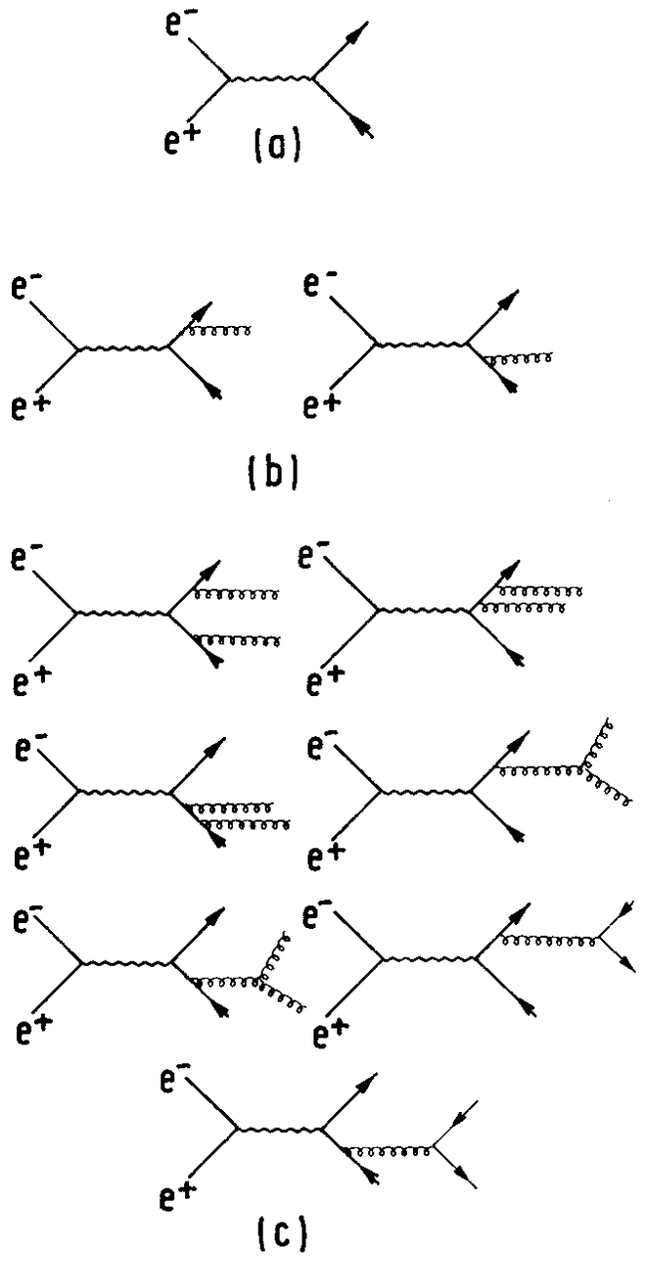

Fig. 1

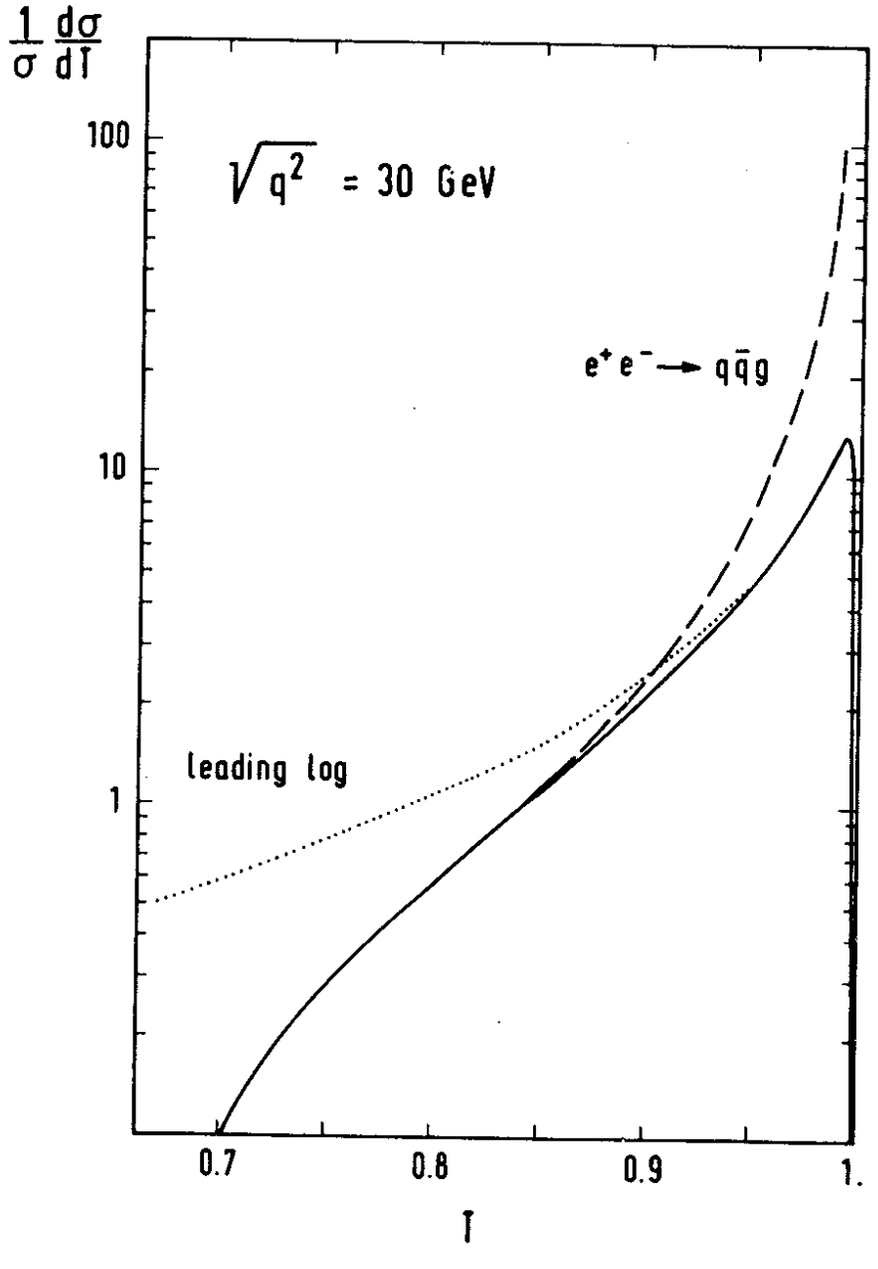
$\frac{1}{\sigma}\frac{d\sigma}{dT}$
100
10
1
$\sqrt{q^2}$ = 30 GeV
$e^+e^- \to q\bar{q}g$
leading log
0.7
0.8
0.9
1.
T

Fig. 2

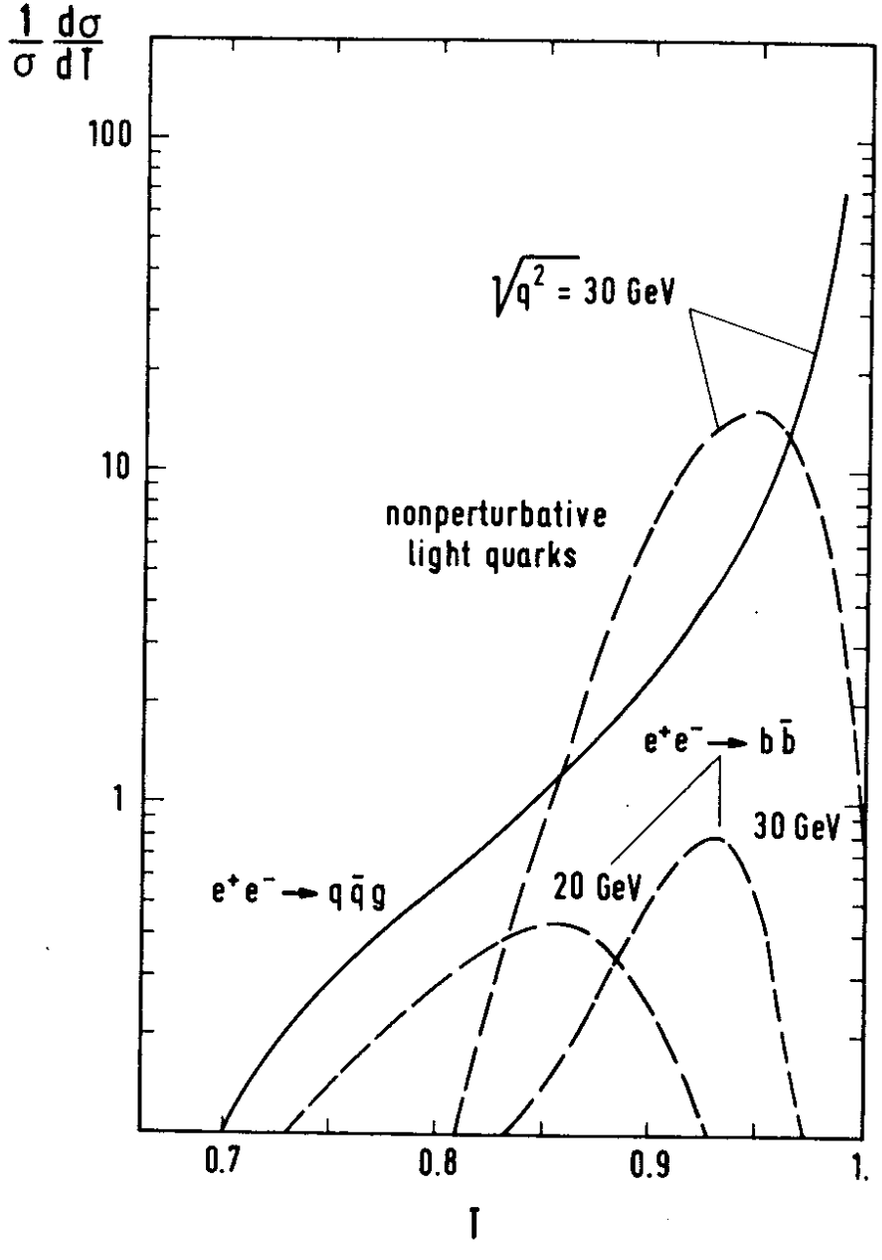
$\frac{1}{\sigma}\frac{d\sigma}{dT}$
100
10
1
$\sqrt{q^2}$ = 30 GeV
nonperturbative
light quarks
$e^+e^- \to b\bar{b}$
30 GeV
20 GeV
$e^+e^- \to q\bar{q}g$
0.7
0.8
0.9
1.
T

Fig. 3

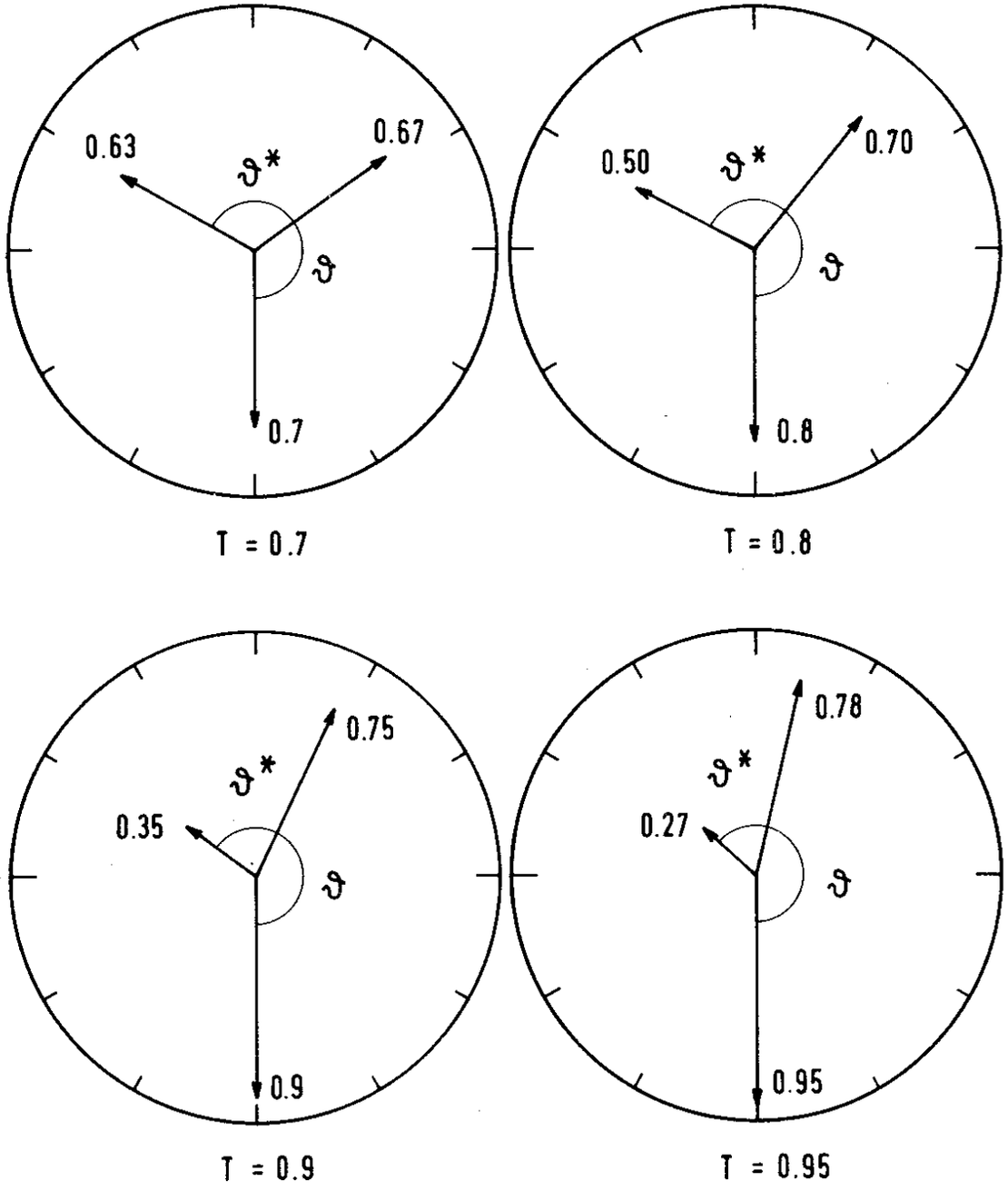
0.63
ϑ*
0.67
ϑ
0.7
T = 0.7
0.50
ϑ*
0.70
ϑ
0.8
T = 0.8
0.35
ϑ*
0.75
ϑ
0.9
T = 0.9
0.27
ϑ*
0.78
ϑ
0.95
T = 0.95

Fig. 4

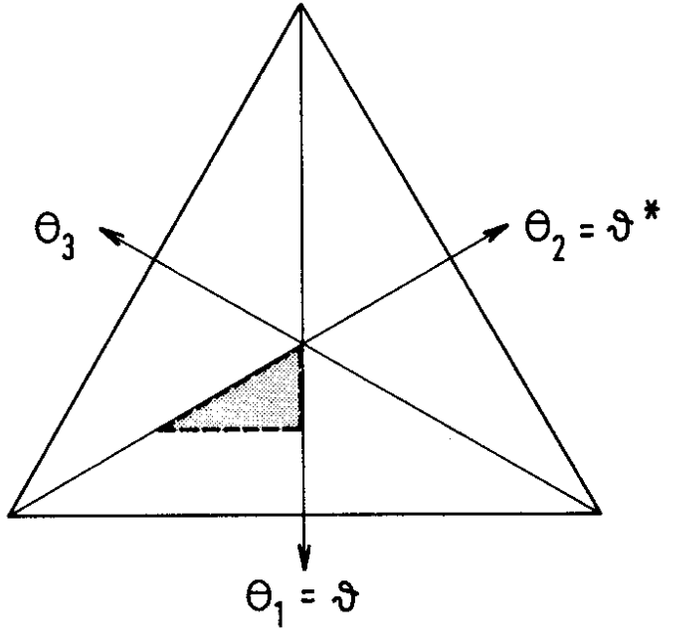
Θ3
Θ2 = ϑ*
Θ1 = ϑ

Fig. 5

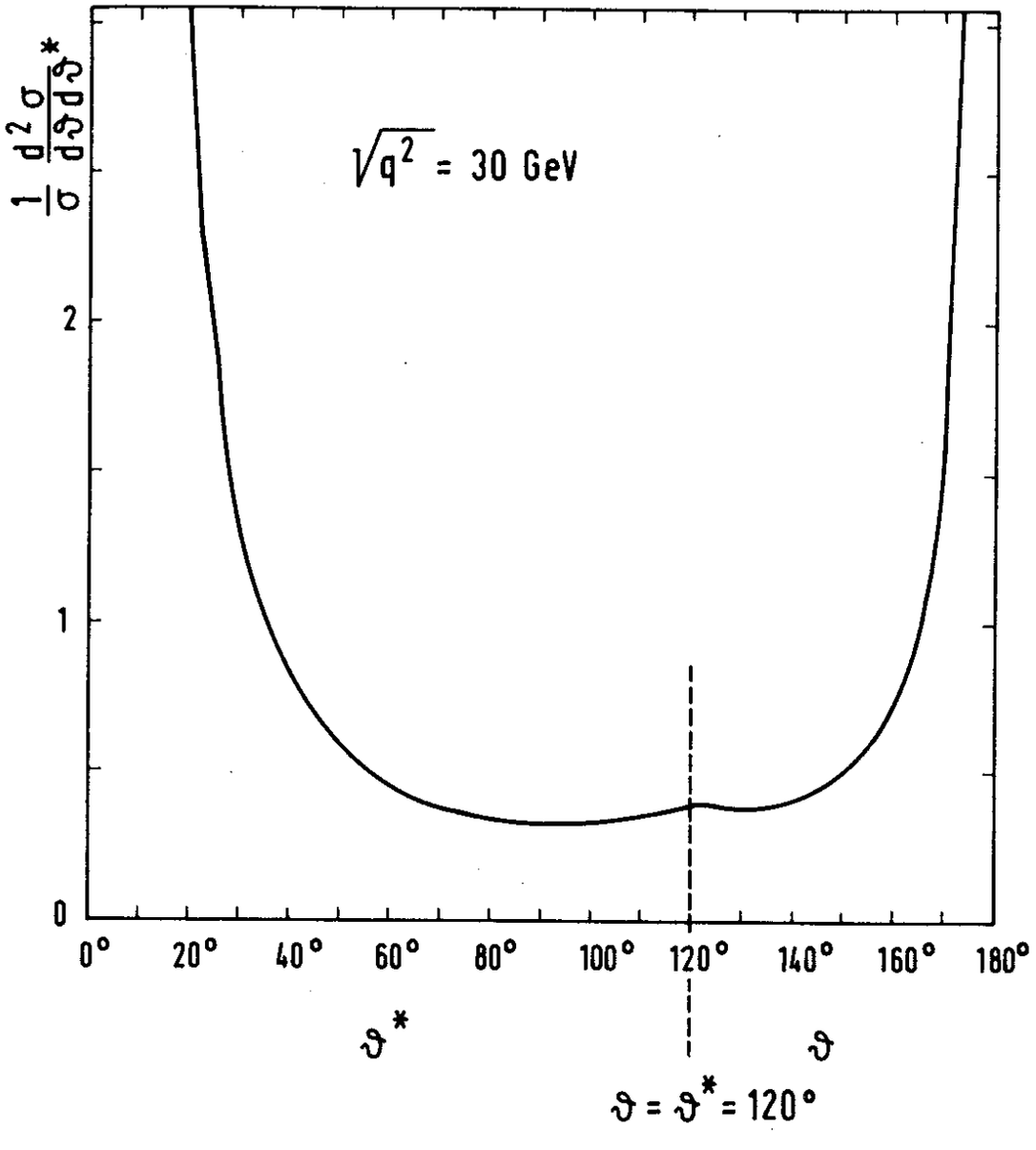
$\frac{1}{\sigma}\frac{d^2\sigma}{d\vartheta d\vartheta^*}$
$\sqrt{q^2}$ = 30 GeV
0
1
2
0°
20°
40°
60°
80°
100°
120°
140°
160°
180°
ϑ^*
ϑ
$\vartheta = \vartheta^* = 120°$

Fig. 6

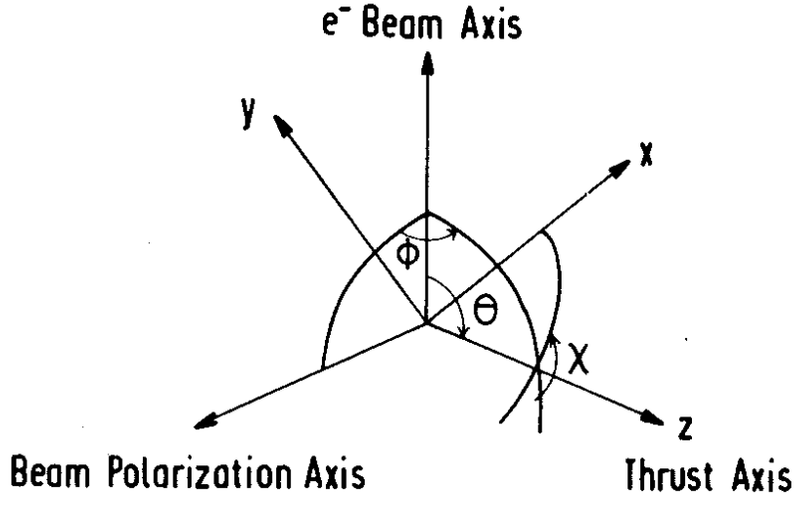
e⁻ Beam Axis
y
x
Φ
Θ
X
z
Beam Polarization Axis
Thrust Axis

Fig. 7

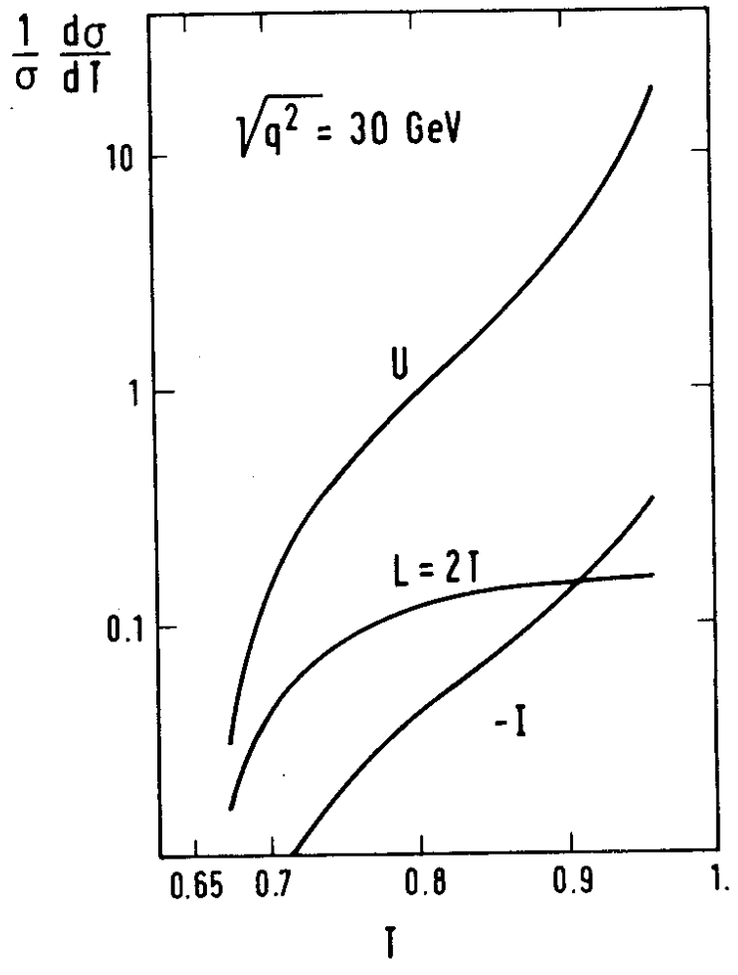
$\frac{1}{\sigma}\frac{d\sigma}{dT}$
$\sqrt{q^2}$ = 30 GeV
10
1
0.1
U
L = 2T
-T
0.65
0.7
0.8
0.9
1.
T

Fig. 8

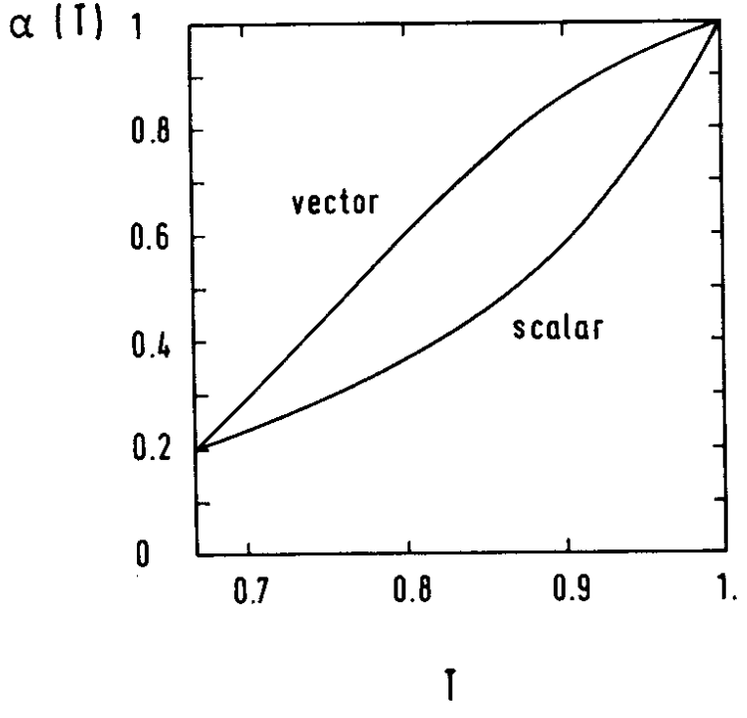
α (T)
1
0.8
0.6
0.4
0.2
0
vector
scalar
0.7
0.8
0.9
1.
T

Fig. 9

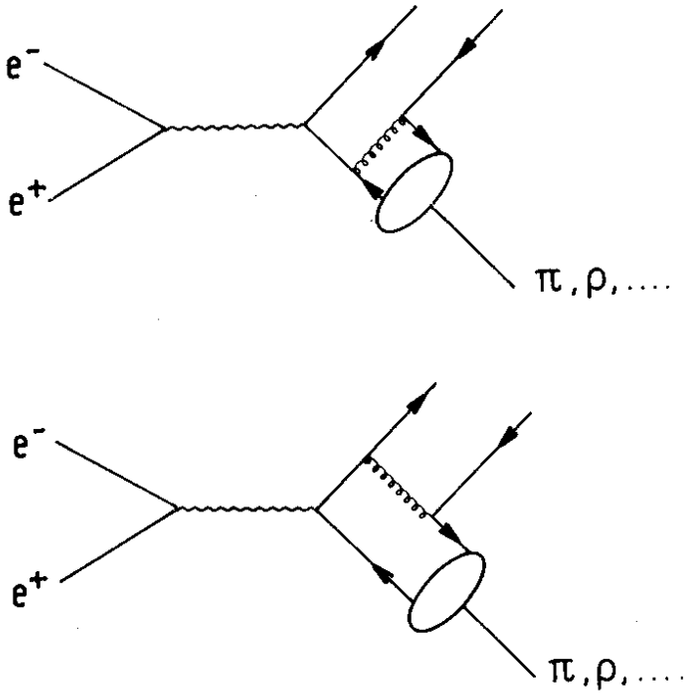
e⁻
e⁺
π, ρ, ...
e⁻
e⁺
π, ρ, ...

Fig. 10

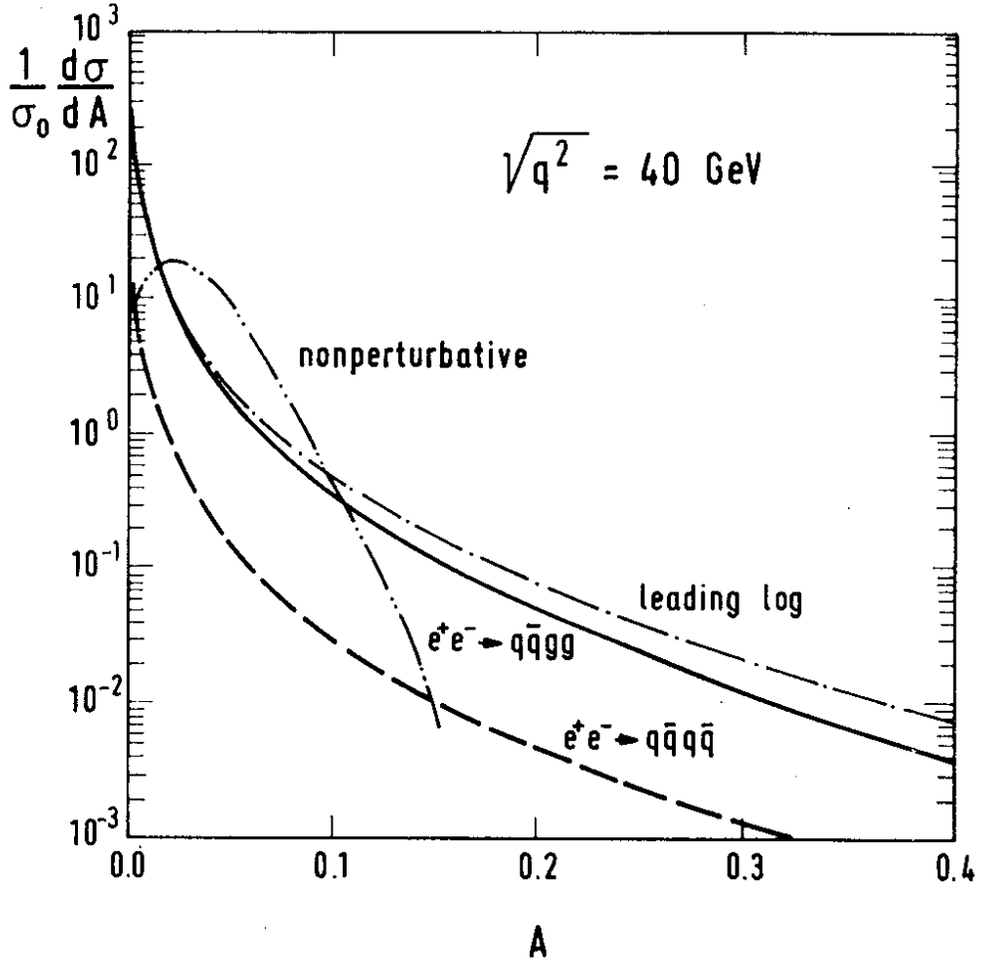
1/σ₀ dσ/dA
10³
10²
10¹
10⁰
10⁻¹
10⁻²
10⁻³
√q² = 40 GeV
nonperturbative
leading log
e⁺e⁻ → qq̄gg
e⁺e⁻ → qq̄qq̄
0.0
0.1
0.2
0.3
0.4
A

Fig. 11

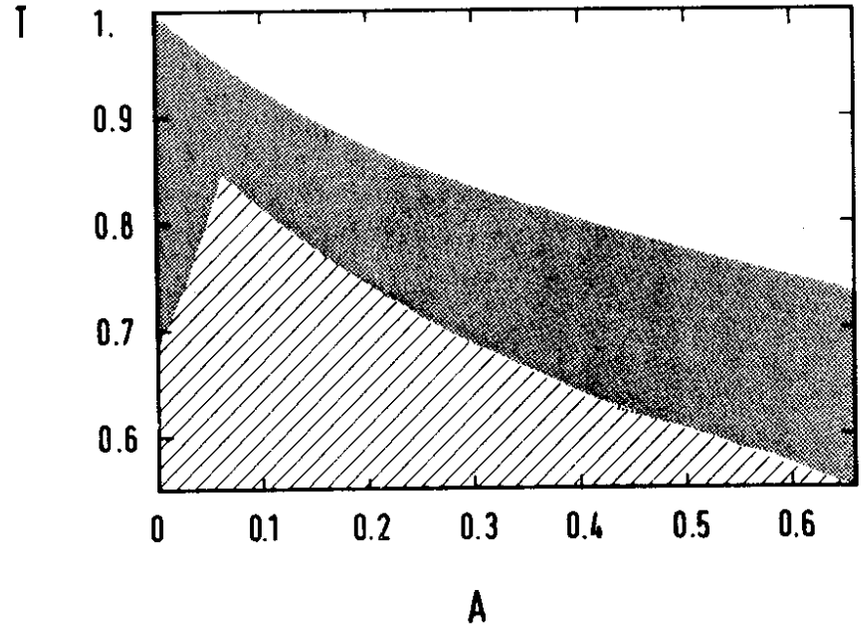
T
1.
0.9
0.8
0.7
0.6
0
0.1
0.2
0.3
0.4
0.5
0.6
A

Fig. 12

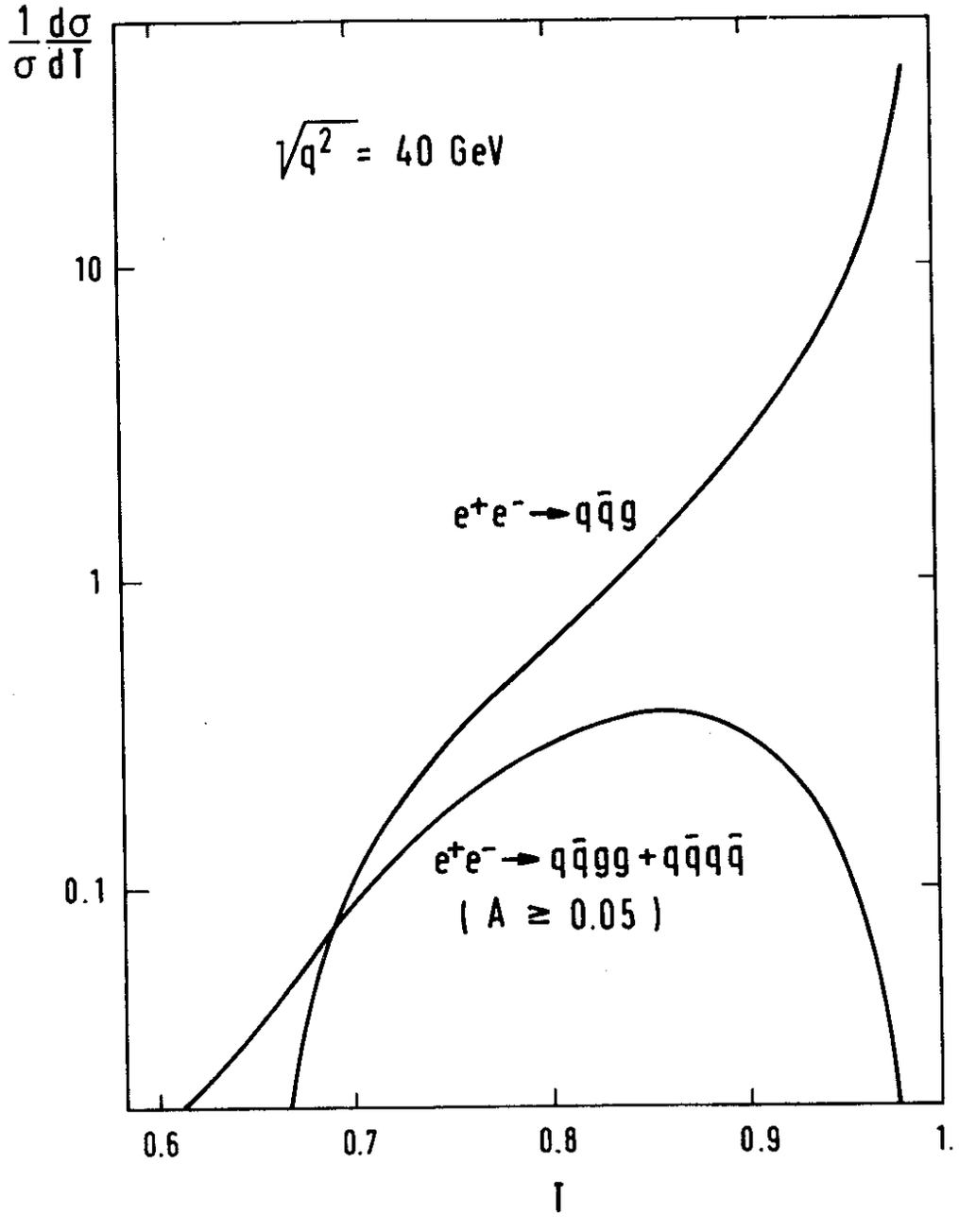
$\frac{1}{\sigma}\frac{d\sigma}{dT}$
$\sqrt{q^2}$ = 40 GeV
10
1
0.1
$e^+e^- \to q\bar{q}g$
$e^+e^- \to q\bar{q}gg + q\bar{q}q\bar{q}$
(A ≥ 0.05)
0.6
0.7
0.8
0.9
1.
T

Fig. 13

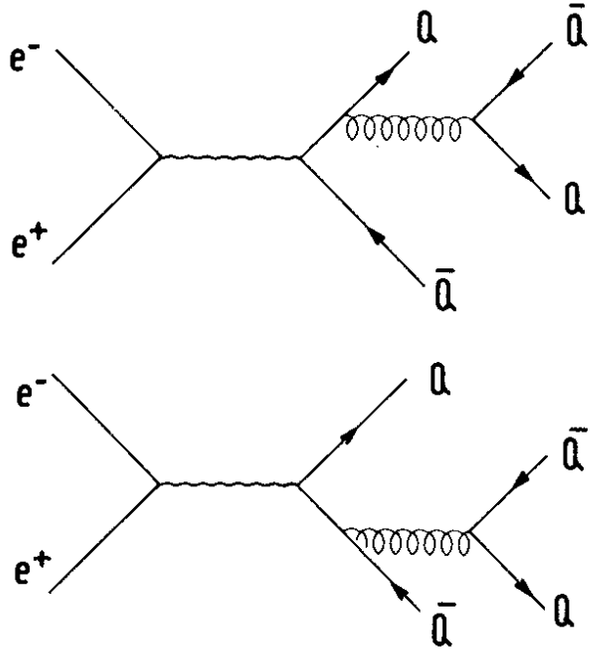

Fig. 14

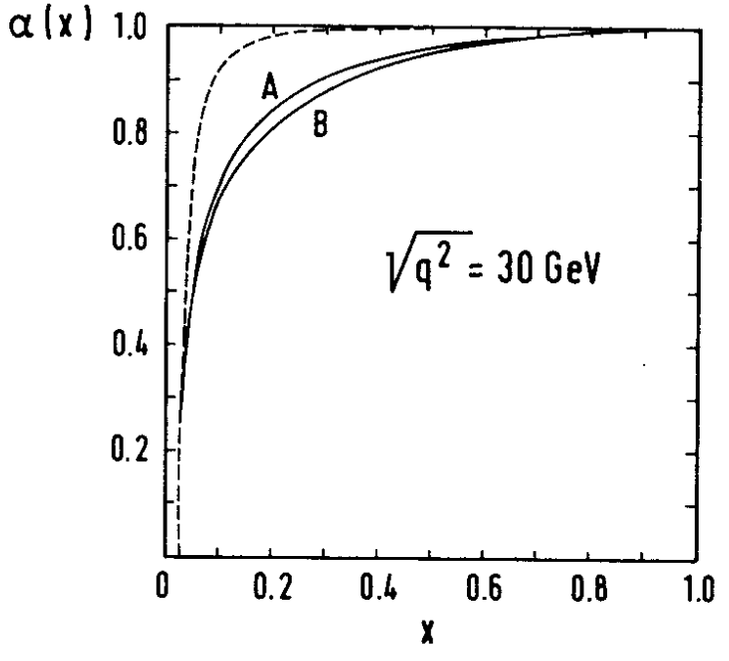

Fig. 15

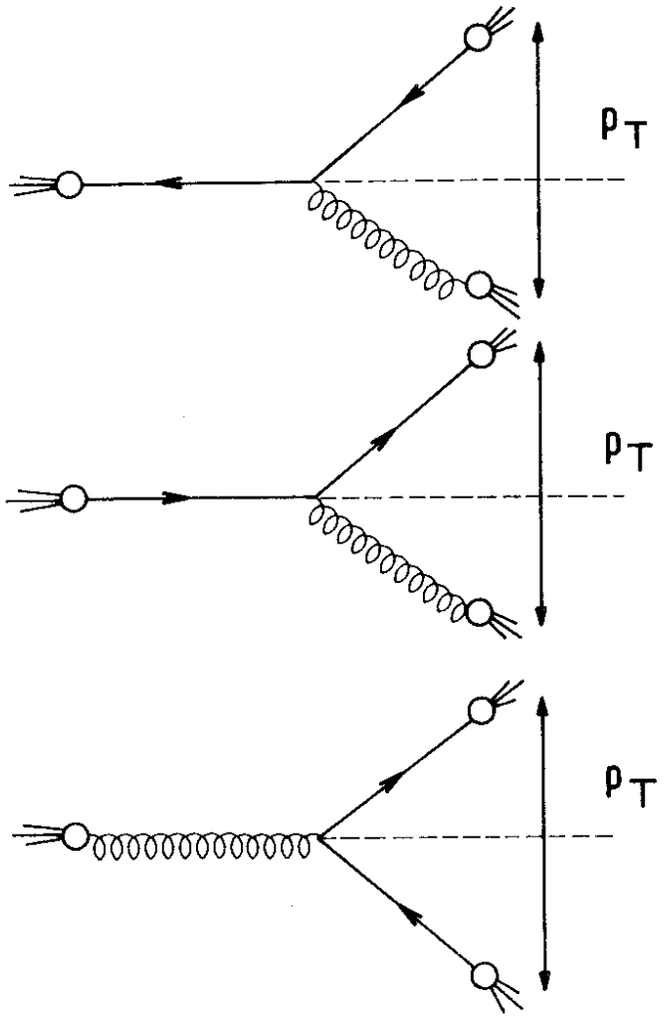
p_T
p_T
p_T

Fig. 16

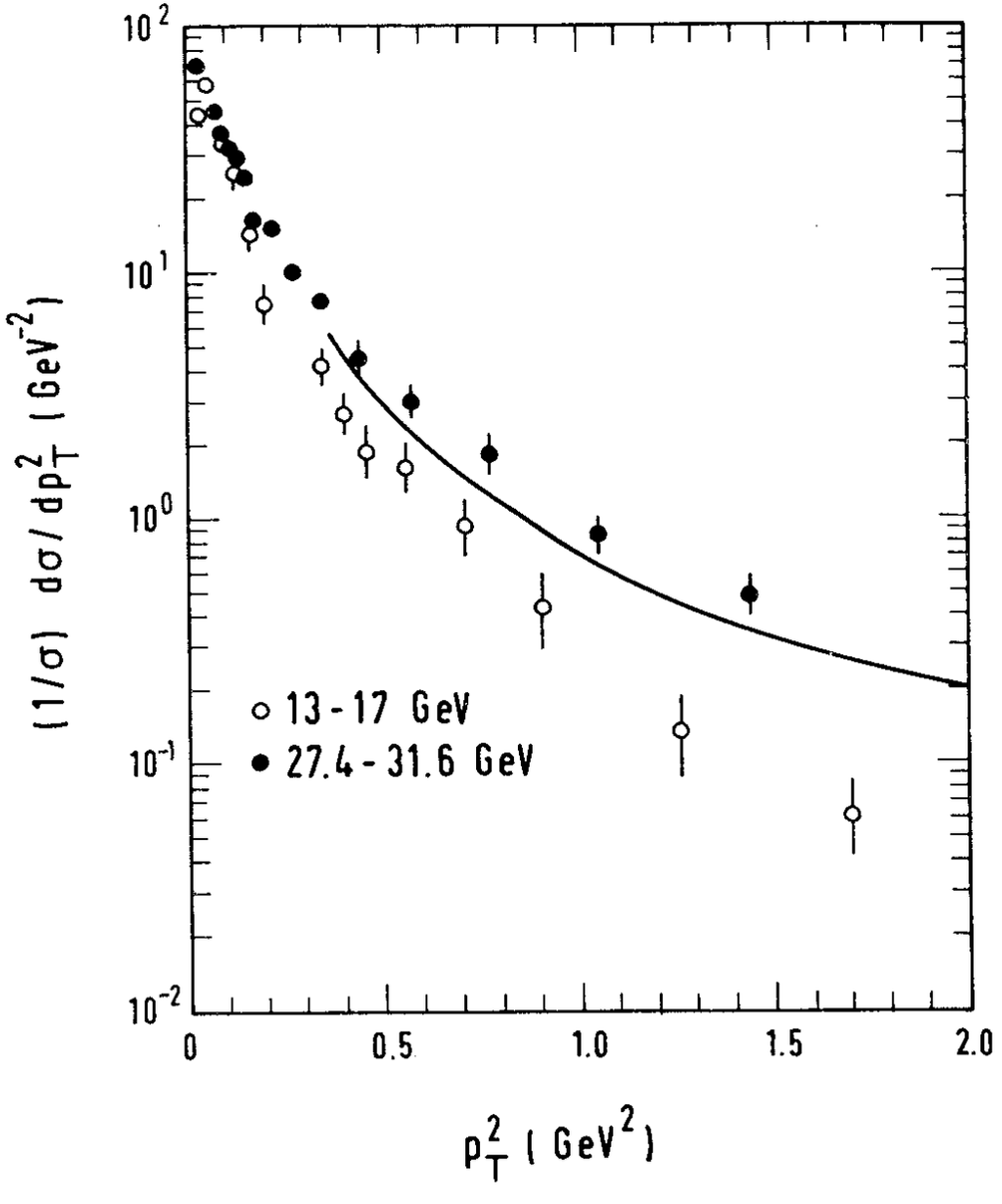
10^2
10^1
10^0
10^{-1}
10^{-2}
$(1/\sigma)\ d\sigma/dp_T^2\ (GeV^{-2})$
○ 13 - 17 GeV
● 27.4 - 31.6 GeV
0
0.5
1.0
1.5
2.0
$p_T^2\ (GeV^2)$

Fig. 17

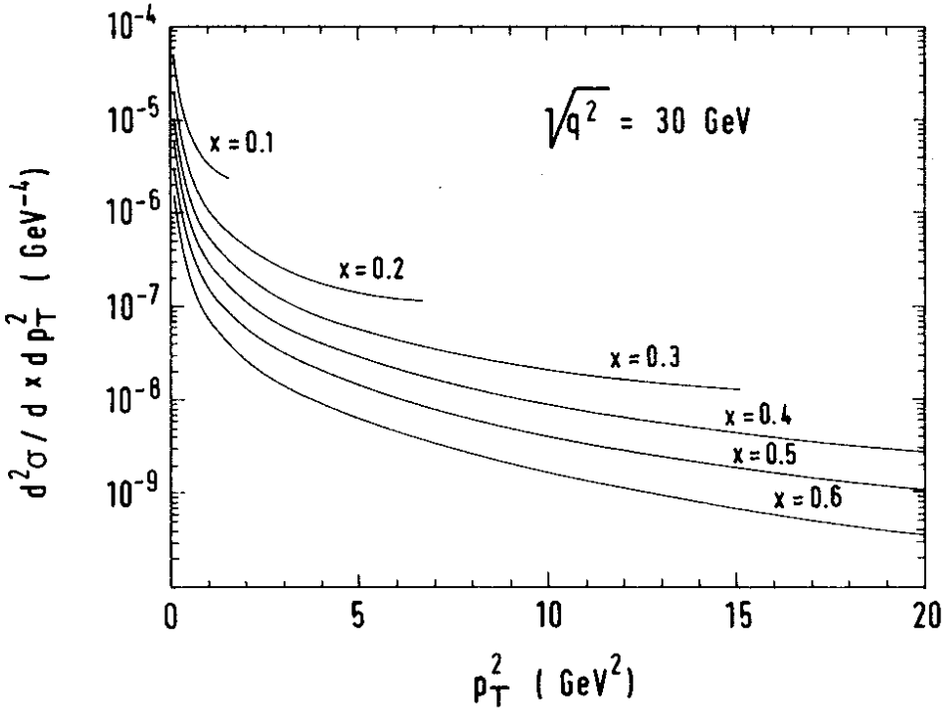

Fig. 18

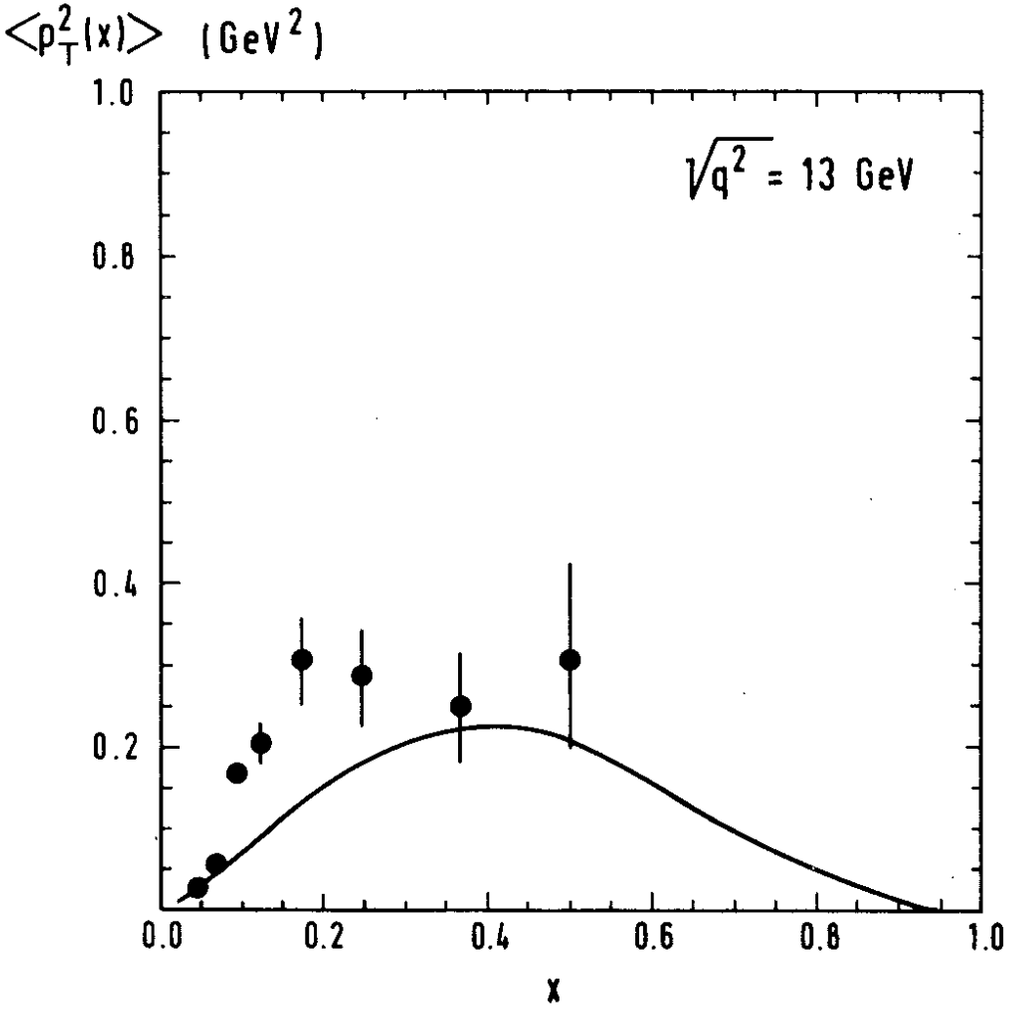

Fig. 19 a

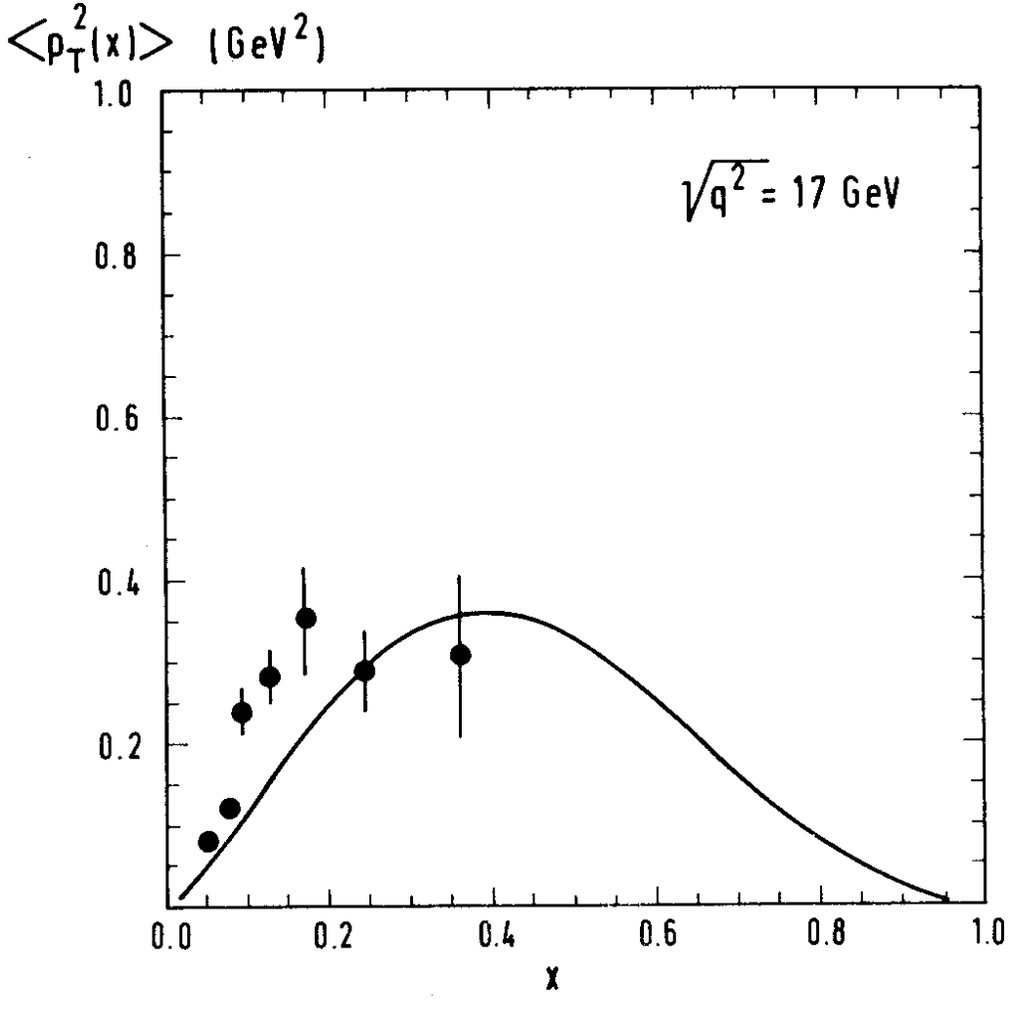

Fig. 19 b

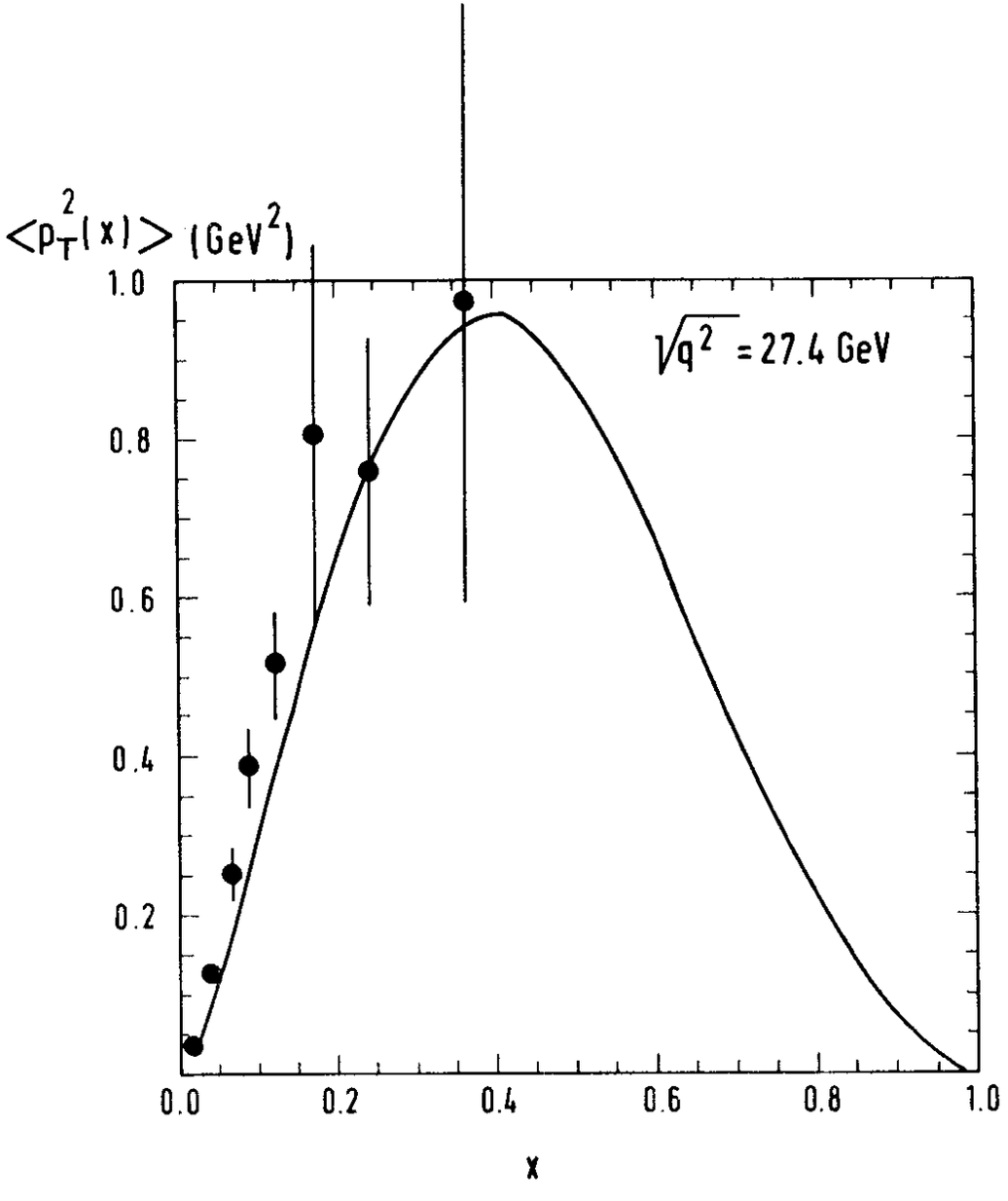

Fig. 19 c

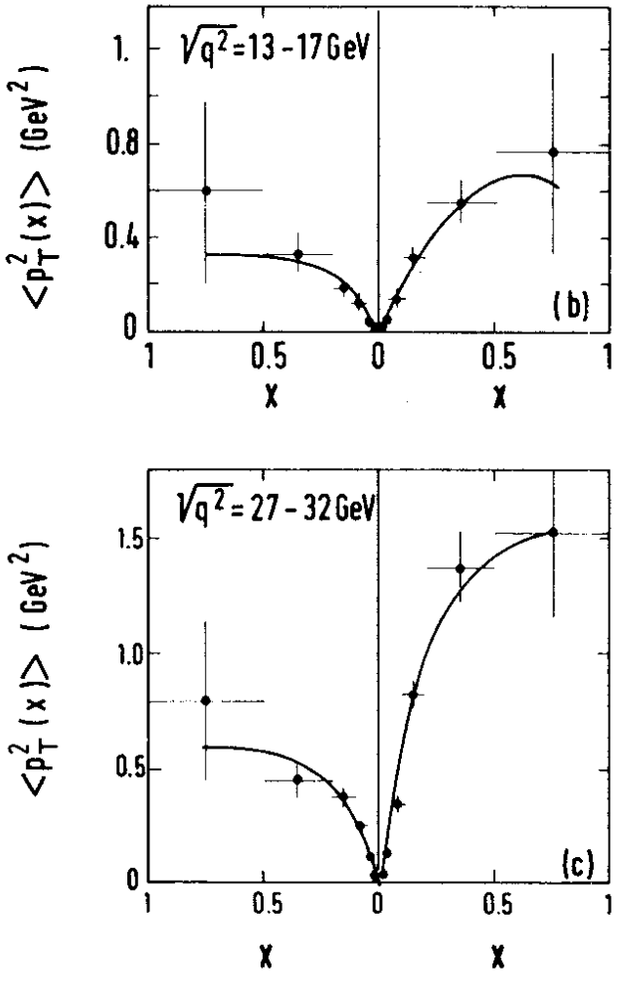
$\sqrt{q^2}$=13 - 17 GeV
(b)
$\sqrt{q^2}$ = 27 - 32 GeV
(c)
$\langle p_T^2(x)\rangle$ (GeV^2)
X

Fig. 20

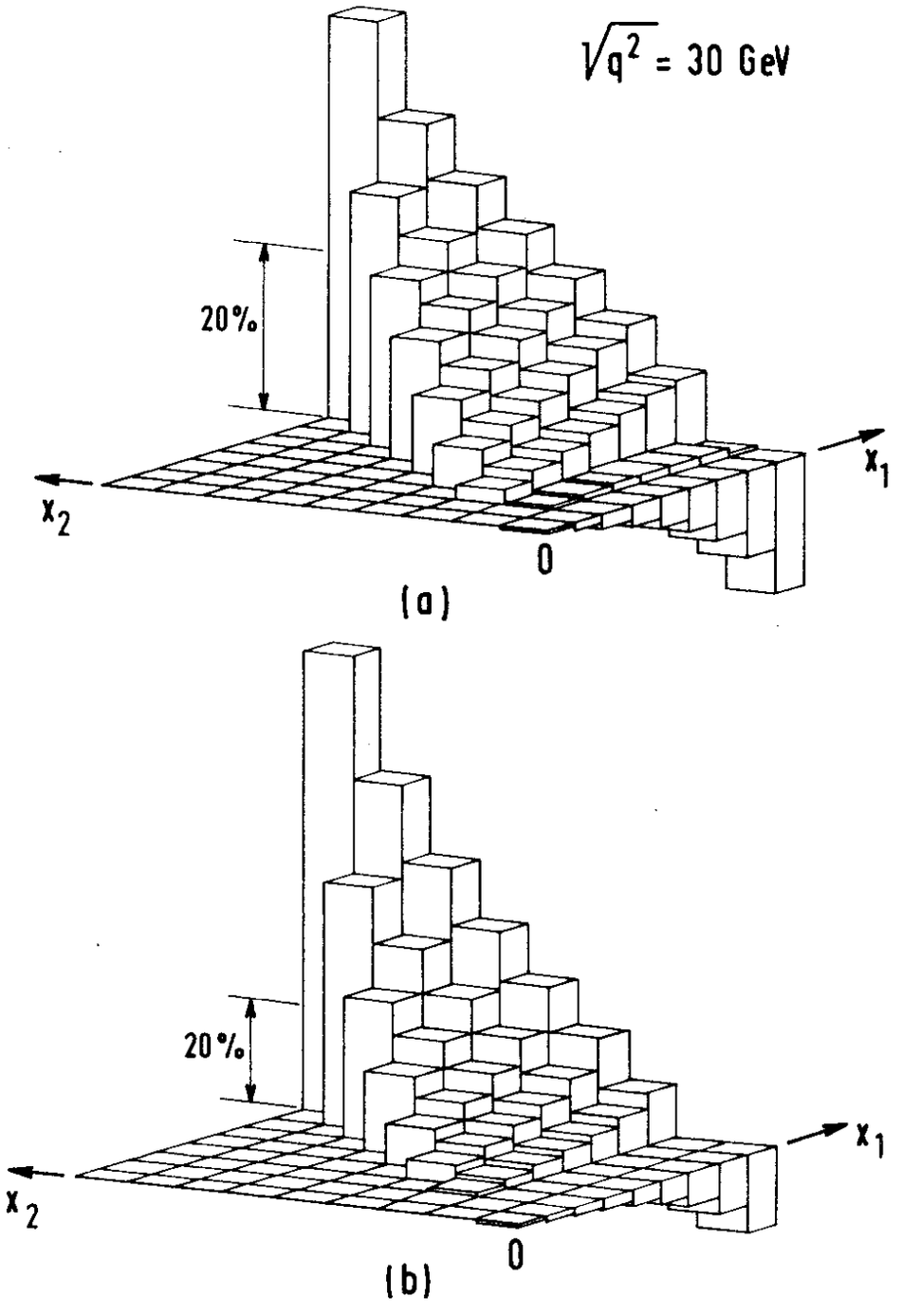
$\sqrt{q^2}$ = 30 GeV
20%
x_1
x_2
0
(a)
(b)

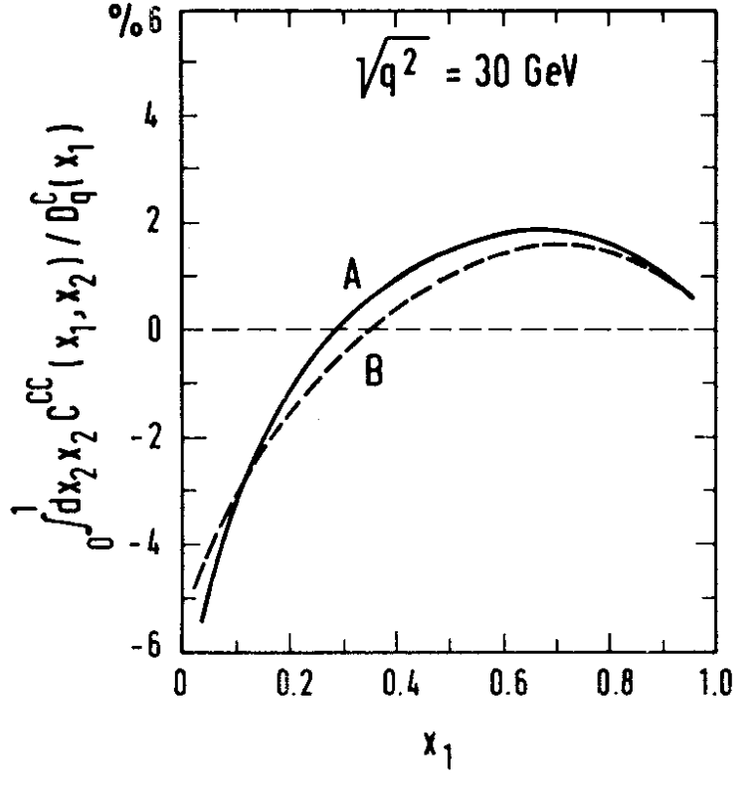
%6
$\sqrt{q^2}$ = 30 GeV
4
2
0
-2
-4
-6
A
B
0
0.2
0.4
0.6
0.8
1.0
x_1
$\int_0^1 dx_2 x_2 C^{cc}(x_1, x_2) / D_q^c(x_1)$

Fig. 22

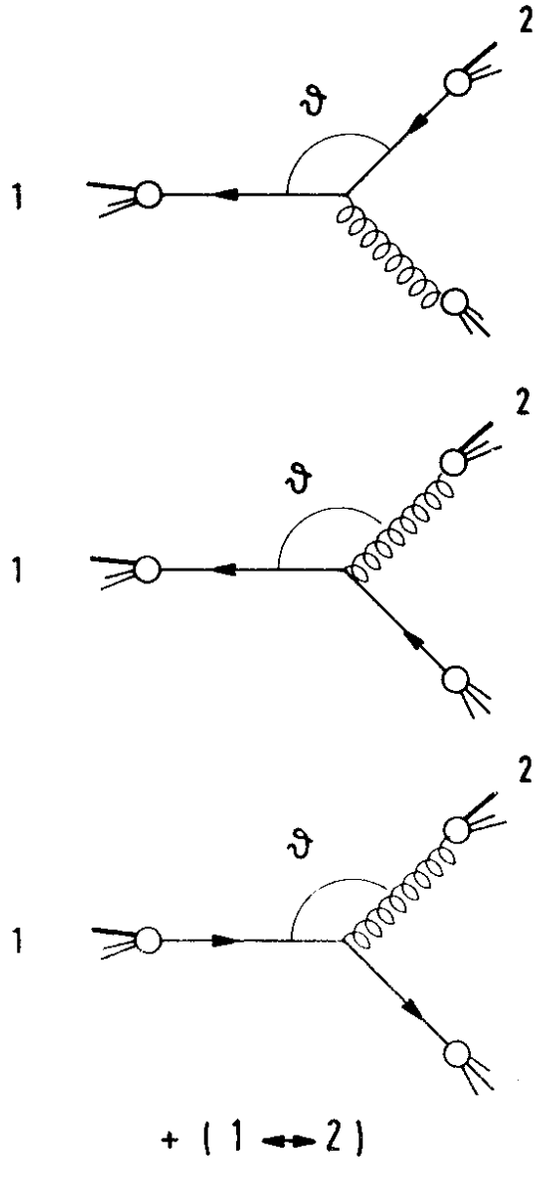
1
2
ϑ
1
2
ϑ
1
2
ϑ
+ (1 ↔ 2)

Fig. 23

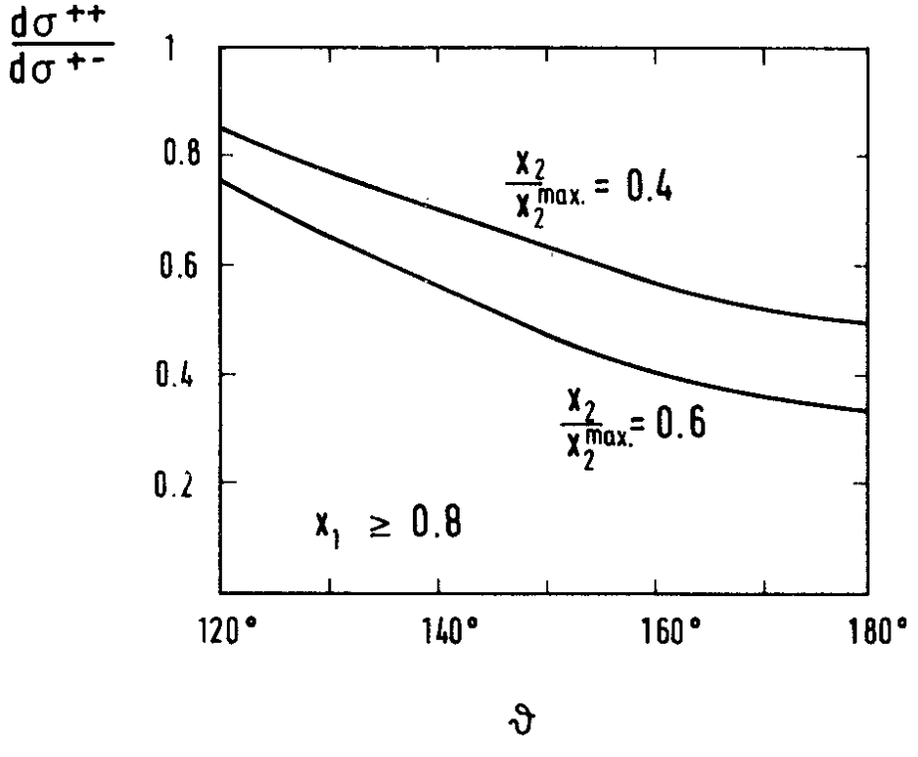
dσ++ / dσ+-
1
0.8
0.6
0.4
0.2
x2 / x2max. = 0.4
x2 / x2max. = 0.6
x1 ≥ 0.8
120°
140°
160°
180°
ϑ

Fig. 24

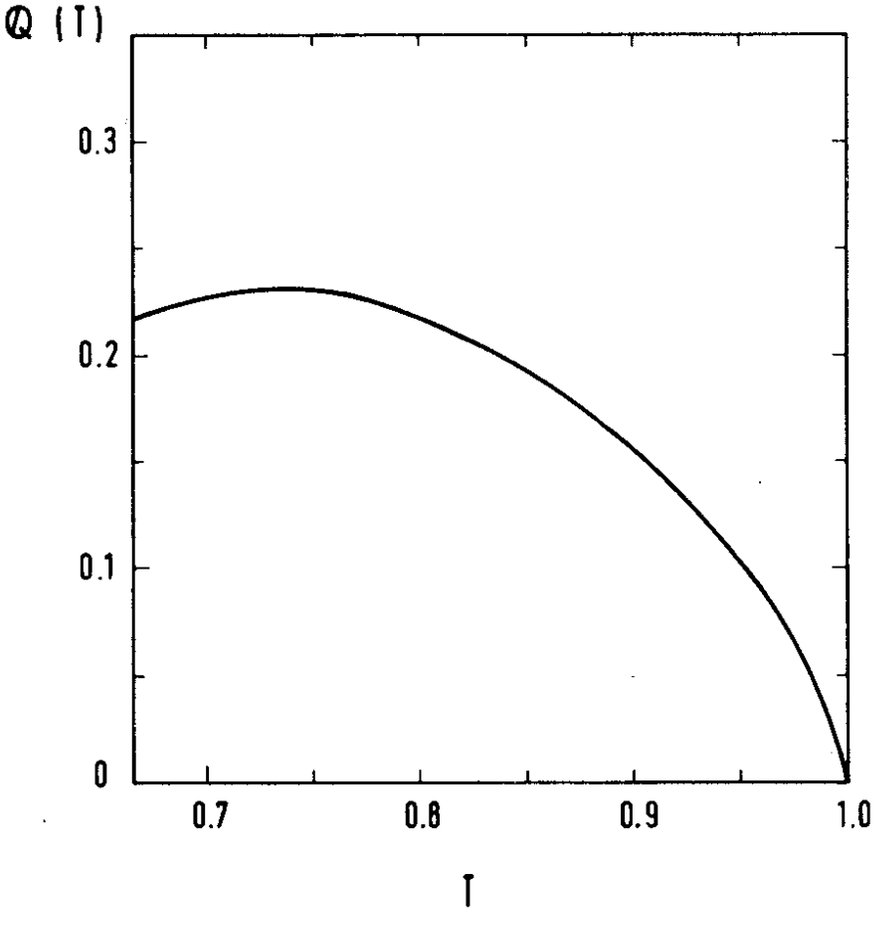
Q (T)
0.3
0.2
0.1
0
0.7
0.8
0.9
1.0
T

Fig. 25